SMALL SCALE TEMPERATURE FLUCTUATIONS NEAR THE SEA SURFACE

Michael Alan Nye Whittemore

NAVAL POSTGRADUATE SCHOOL
Monterey, California

THESIS

SMALL SCALE TEMPERATURE FLUCTUATIONS
NEAR THE SEA SURFACE

by

Michael Alan Nye Whittemore

Thesis Advisor: Noël Boston

March 1973

Small Scale Temperature Fluctuations Near The Sea Surface

by

Michael Alan Nye Whittemore
Lieutenant, United States Navy
B.S., U.S. Naval Academy, 1966

Submitted in partial fulfillment of the
requirements for the degree of

MASTER OF SCIENCE IN OCEANOGRAPHY

from the

NAVAL POSTGRADUATE SCHOOL
March 1973

ABSTRACT

Thermistor measurements of small scale temporal and spatial fluctuations of temperature were made near the surface of the sea from the NUC Oceanographic Research Tower. Wave height, water particle velocity, sound velocity, and salinity were measured simultaneously. Data were subjected to statistical and spectral analyses. Temperature fluctuations were found to vary with wave height. A linear relation was found to exist between temperature fluctuations and wave swell. The assumed relationship was verified by the results of spectral analysis. High coherence (.68) between wave height and temperature fluctuations occurred near the frequency of maximum wave energy. A relatively constant phase difference of 180^{o} was observed in the frequency band normally associated with surface swell (.03 Hz to 0.2 Hz). Water particle velocities displayed the same relatively high coherence in the frequency band of high wave energy. Temperature fluctuations were 180^{o} out of phase with the u-component of velocity and 90^{o} out of phase with the w-component of velocity. These phase differences agreed with linear wave theory. Coherence was observed to be lower and phase difference more random with increased thermal gradients. This was attributed to an increase in turbulent temperature fluctuations.

TABLE OF CONTENTS

LIST OF TABLES

LIST OF FIGURES

LIST OF FIGURES (continued)

ACKNOWLEDGEMENT

The author wishes to thank Professor Noël E. J. Boston and Professor Edward B. Thornton for their guidance in the development of this thesis, and especially for their patience and understanding during the many discussions necessary in bringing this work to a successful end.

I. INTRODUCTION

An experiment designed to measure fluctuations of environmental parameters in a small volume of water near the surface of the sea was conducted on 8 and 9 June, 1972. The experiment was carried out on the Naval Undersea Research and Development Center's Oceanographic Research Tower in San Diego, California by members of the Oceanography Department, U. S. Naval Postgraduate School.

The main objectives of the portion of the experiment described herein were to:

1. Measure the spatial and temporal temperature field,

2. Define a relationship that describes the temperature field in the near surface ocean,

3. Examine the relationships between the temperature field and other measured parameters via spectral and statistical analyses.

Temperature in the ocean environment may be regarded as a passive scalar. Passive scalars are quantities, including contaminants, that modify and/or can be transported in a fluid but which do not introduce bouyancy effects. A scalar which introduced bouyancy effects would be considered to be active. Clearly large temperature differences can result in bouyant motion but the scales of temperature fluctuations considered here render such induced motion negligible.

Since temperature is a passive scalar, the temperature field does not create motion but responds to motion. The temperature field is advected and convulsed by the vector velocity field. The temperature

field is then expected to reflect changes and motion occurring within the velocity field. As such it is a good indicator of the types of motion occurring in the near surface ocean.

Temperature change can be caused by:

1. the vertical motion of the temperature gradient with negligible changes to the gradient,

2. the movement of a continuum mass of water with distinctive temperature structure,

3. wave induced motion,

4. turbulence.

The first of these usually result from internal waves, which can occur whenever a density gradient exists in the fluid. Internal wave motion can be irrotational, linear, and not alter the mean temperature gradient. However non-linear internal wave motions do exist and can induce large changes in the temperature gradient. A large body of literature on internal waves exists and it is not intended to discuss the manifold variety of these waves in this paper. Only motions pertinent to this experiment will be examined in order to interpret results of the experiment.

The second cause of temperature fluctuations is due to water with a different temperature field being advected past the point of interest, which would include such things as currents and large eddies. The contributions from this source are considered to be negligible in the area of this experiment.

Wave induced temperature fluctuations are limited to depths where wave motion is in evidence which normally encompasses depths of less than one wave length. Furthermore, in order for wave action to cause

temperature fluctuations, temperature inhomogeneities must be present in the water which surrounds a fixed temperature sensor.

Oceanic turbulence is a broad band phenomenon covering scales of kilometers to fractions of a centimeter. It is thus present to modify temperature fluctuations caused by each of the above three processes. At scales sufficiently removed from those of other processes, the temperature field itself can be considered to be a turbulent field which, analogous to the velocity field, has an "energy" containing region and an inertial sub-range. Due to the difference in the rates of viscous and thermal dissipation in the ocean, the very small scale temperature field tends to persist longer than the velocity field and, thus, water which was at one time turbulent can be "marked" by a turbulent temperature field. Although such small scales are beyond the scope of the apparatus used for this experiment, turbulence at larger scales will be examined.

In order to meet the objectives proposed by this thesis, it is necessary to be able to separate the various causes of temperature fluctuations. Fortunately this is not difficult in the case of internal and surface waves. These tend to have narrow spectra and appreciable energy. Furthermore they are well separated from each other. At the experimental site, internal waves tend to be present at periods from 4-10 minutes whereas a typical surface wave period is several seconds. Resolution of advected temperature fluctuations is more difficult as many scales are involved. A prior model of the temperature field must be assumed and several sensors are needed to adequately define horizontal and vertical scales.

The time scale, length scale, measuring device used, and environmental conditions all effect the components that will be present in the measured Eulerian temperature signal. The length of the longest data record in this experiment was about 25 minutes, the spatial separation of sensors ranged from 23 centimeters to 89 centimeters and sea surface conditions were restricted to swell-type waves. The above conditions thus restricted the main causes of temperature fluctuations to:

1. Internal waves
2. Surface swell
3. Small scale turbulence

Internal waves are gravity waves that can exist whenever a density gradient exists in a fluid. In the ocean, these waves propagate along thermal gradient layers where the vertical change in density is very small compared to the average density in the water column. Under these conditions it is possible to have very long internal waves with large amplitudes propagate with only a small amount of energy. Internal waves are most often manifested in oceanographic data as Eulerian temperature fluctuations. Typical internal waves for the area of this experiment have been described in the literature [Lafond,(7)]. He found periods ranging from four to eight minutes, amplitudes from 60 to 240 cm., and an average velocity of about 15 cm./sec. The temperature fluctuations associated with internal waves should exhibit a linear relationship with the instantaneous wave amplitude of the internal wave at the depth under consideration and the temperature gradient. If $A_o(t)$ is the instantaneous amplitude of the internal wave at the depth under consideration, Z_o, then a reasonable expression for temperature fluctuations due to internal wave propagation is:

$$T_{IW}(t) = \frac{dT}{dz} \cdot A_o(t) \qquad \text{(I-1)}$$

Surface swell is known to be closely approximated by linear theory. The waves for this study were analyzed [Krapohl,(6)] and found to obey linear theory to a high degree of accuracy and thus can be considered to be linear and irrotational. If $\eta(t)$ is the instantaneous wave height, then the temperature fluctuations due to surface swell should be of a form similar to those due to internal waves:

$$T_W(t) = K(z,f) \cdot \frac{dT}{dz} \cdot \eta(t) \qquad \text{(I-2)}$$

where $K(z,f)$ is a constant that relates the motion at the surface to the motion of the water column at the depth under consideration. Surface swell has periods ranging from 6 to 20 seconds and amplitudes on the order of meters. Furthermore, from equations (I-1) and (I-2), it is clear that in the presence of a negative temperature gradient the temperature fluctuations will be 180^{o} out of phase with the instantaneous amplitude of internal and surface waves.

The separation of the turbulent temperature signal from the total signal at first appears quite difficult. Certainly deterministic approaches have not been successful in turbulence studies and statistical treatments are often followed. However because of the narrowness of internal and surface wave spectra the dominating cause of temperature fluctuations is usually recognizable. Furthermore the "energy" contained in turbulent temperature fluctuations is quite small which means that at frequencies where internal or surface waves are found, turbulence is not a major feature.

In order to determine clearly the relationships between the various parameters measured during this experiment, it is desirable to remove the effects of turbulence, even if they are small, from the signals of the other parameters. Spectral analysis partially aids us in this direction but additional analysis schemes need to be investigated. Necessarily such schemes will be band limited to cover the scales the experiment is able to resolve. For this experiment, the turbulent frequency range would be from about 0.5 Hz on up to the Nyquist frequency.

Figure (1) displays a qualitative prediction of the thermal energy density distribution that could reasonably be expected under the constraints of this experiment. As has been discussed, where surface swell and internal waves predominate, there are also "masked" contributions from turbulent processes.

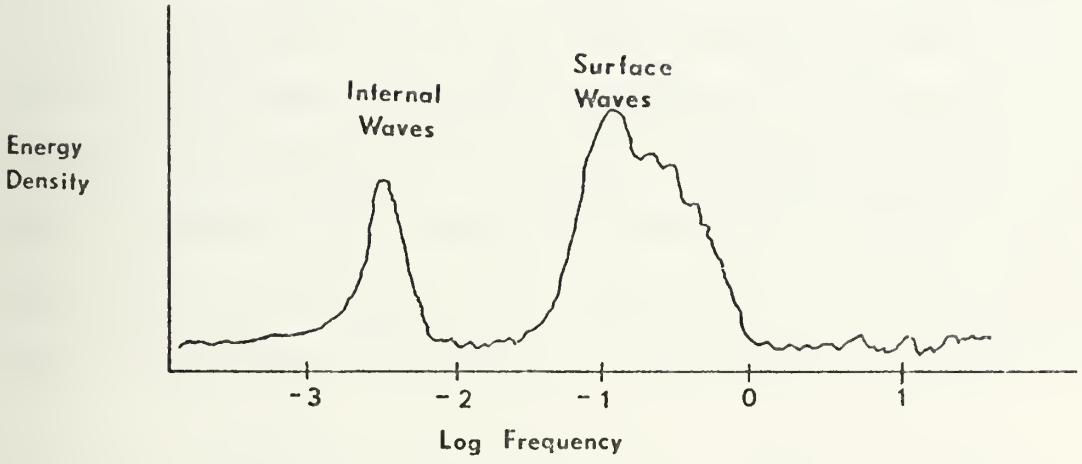

Figure 1. Predicted energy density distribution of temperature fluctuations.

II. THEORETICAL CONSIDERATIONS

Discussions of random data analysis schemes are found in many references. The following discussion is based, in large part, on chapters 3,5,6 and 9 of Bendat and Piersol's Random Data, Analysis and Measurement Procedures. Throughout this discussion temperature fluctuations due to all causes are assumed to be stationary and independent from one another.

Temperature fluctuations due to surface swell can be described by a constant parameter linear system whose fundamental properties are invariant with time. The dynamic characteristics of this type of system can best be described through the use of a weighting function, $h(\tau)$, which is defined as the output of a system at any time to a unit impulse applied at a time τ before. The output, $T(t)$, of this system whose input is surface wave height, $\eta(t)$, is given by the convolution integral:

$$T(t) = \int_0^\infty h(\tau) \cdot (t - \tau)d\tau \qquad \text{(II-1)}$$

The Fourier transform of the weighting function is the transfer function defined by:

$$H(f) = \int_0^\infty h(\tau)e^{-i2\pi ft}d\tau \ ; \qquad \text{(II-2)}$$

where f is frequency. From equation (II-1) it can easily be shown that:

$$T(t + \tau) = \int_0^\infty h(\tau)\eta(t + \tau - \zeta)d\zeta \ ; \qquad \text{(II-3)}$$

where ζ is a dummy variable.

The product of $T(t)$ and $T(t + \tau)$ is given by:

$$T(t) \cdot T(t + \tau) = \int_0^\infty \int h(\zeta)\eta(t - \zeta) \cdot h(\epsilon)\eta(t + \tau - \epsilon)d\epsilon d\zeta \; ; \qquad \text{(II-4)}$$

where ζ and ϵ are dummy variables.

The time average of the above equation is defined as the temporal auto-covariance function, $R_T(\tau)$. In terms of weighting functions and the input auto-covariance function, $R_T(\tau)$ is given by:

$$R_T(\tau) = \int_0^\infty \int h(\epsilon)h(\zeta)R_\eta(\tau + \epsilon - \zeta)d\epsilon d\zeta \qquad \text{(II-5)}$$

The cross-covariance function between the input and output can similarly be derived using as a starting point the relation:

$$\eta(t) \cdot T(t + \tau) = \int_0^\infty h(\epsilon)\eta(t) \cdot \eta(t + \tau - \epsilon)d\epsilon \qquad \text{(II-6)}$$

which yields on time averaging the cross-covariance relation:

$$R_{\eta T}(\tau) = \int_0^\infty h(\epsilon)R_\eta(\tau - \epsilon)d\epsilon \qquad \text{(II-7)}$$

The Fourier transform of the auto-covariance function is related to the spectral energy-density function by the relation:

$$S_T(f) = 4\int_0^\infty R_T(\tau) \cos(2\pi f\tau)d\tau \qquad \text{(II-8)}$$

The Fourier transform of the cross-covariance function is similarly related to the cross-spectral energy density function by the relation:

$$S_{\eta T}(f) = \int_{o}^{\infty} R_{\eta T}(\tau) e^{-i2\pi ft}\, d\tau \qquad \text{(II-9)}$$

From equations (II-2),(II-8), and (II-9) two important equations in the frequency domain can be derived:

$$S_T(f) = \left|H(f)\right|^2 \cdot S_\eta(f) \qquad \text{(II-10)}$$

and:

$$S_{\eta T}(f) = H(f) \cdot S_\eta(f) \qquad \text{(II-11)}$$

In the frequency band of swell waves (about .05 Hz to .3 Hz) temperature fluctuations are composed primarily of fluctuations due to surface waves, T_W, and fluctuations due to turbulence, T_t. Thus the temporal temperature field, T(t), can be linearly expressed as:

$$T(t) = T_W(t) + T_t(t) \qquad \text{(II-12)}$$

It is assumed that the wave induced and turbulent temperature fluctuations are statistically independent. The spectral energy density function of the temperature fluctuations is then given by:

$$S_T(f) = S_{T_W}(f) + S_{T_t}(f) \qquad \text{(II-13)}$$

The coherence function, $\gamma^2_{12}(f)$, between wave height and temperature is defined by:

$$\gamma^2_{\eta T}(f) = \frac{\left|S_{\eta T}(f)\right|^2}{S_\eta(f) \cdot S_T(f)} \qquad \text{(II-14)}$$

Assuming that T_W and T_t are statistically independent implies that:

$$S_{\eta T}(f) = S_{\eta T_W}(f) \qquad \text{(II-15)}$$

If it is further assumed that the temperature fluctuations due to waves can be expressed as a constant parameter linear system with wave height as the input, then clearly the coherence between wave height and temperature should be equal to one:

$$\gamma^2_{\eta T_W}(f) = \frac{\left|S_{\eta T_W}(f)\right|^2}{S_{T_W}(f) \cdot S_\eta(f)} = 1 \qquad \text{(II-16)}$$

Substituting equations (II-13), (II-15) and (II-16) into equation (II-14) and simplifying yields:

$$\gamma^2_{\eta T}(f) = \left(1 + \frac{S_{T_t}(f)}{S_{T_W}(f)}\right)^{-1} \qquad \text{(II-17)}$$

The assumption that the turbulence- and wave- generated temperature fluctuations are statistically independent and uncorrelated allows us to arrive at equation (II-17). Allowing correlation between the two variables would add to the complexity but would still yield the same basic result and thus the simplification is preferred for discussion purposes.

From equation (II-17) it can be seen that turbulence-generated temperature fluctuations, which can be considered as noise in the process, cause the coherence between wave height and temperature fluctuations to be less than one. Furthermore it is also obvious that if the spectrum of wave generated temperature fluctuations is held nearly constant then an increase in turbulence will cause the coherence between wave height and temperature fluctuations to become smaller.

If the assumed relationship between surface waves and temperature fluctuations is correct, i.e.;

$$T_W(t) = K(z,f) \cdot \frac{dT}{dz} \cdot \eta(t) \qquad \text{(II-18)}$$

then we would expect that in the absence of turbulence the coherence function would reach a value of one at the frequency of the predominant swell and furthermore that in the presence of a negative vertical temperature gradient we should find a phase angle between waves and temperature fluctuations of 180^{o}.

Further, it should be noted that if turbulent temperature fluctuations are present then the coherence will be less than one as shown by equation (II-17). Also turbulence would be expected to modify the phase angle to some extent in a more or less random fashion.

III. INSTRUMENTATION

The temperature sensing device chosen for this experiment was the type K496 double beaded thermistor manufactured by Fenwall Electronics Inc., Framingham, Massachusetts. This thermistor has an exceptionally thin glass coating which provides a water-tight covering and allows for a low thermal response time of less than 150 milliseconds. The resistance of the thermistor is about 18 K-ohms at 20° C and varies about 870 ohms per 1° C in the temperature range from 16° C to 22° C. These high resistance values give the thermistor a high degree of resolution. The thermistor also has very low self-heating and thus in seawater can provide temperature measurements accurate to $.01^{\circ}$ C. Further details on the type K496 can be found in reference (10).

The thermistor was supplied mounted with epoxy potting compound in a 3mm diameter hollow steel tube. The leads of the thermistor, which extended from the tube, were soldered to plastic-coated, shielded instrumentation cable. This connection and the end of the steel tube were placed in a mold which was then filled with epoxy potting compound. On hardening, the epoxy formed a 6 cm in diameter base for the steel tube which protruded about 9 cm above the base. The overall sensor length was about 14 cm. A total of six sensors were prepared and calibrated in a temperature controlled bath using a previously calibrated digital quartz thermometer over the range from 10° C to 22° C. A typical temperature versus resistance calibration curve is shown in Figure (2). For any small temperature range ($\pm$ 2° C) the curve is linear to a high degree of accuracy.

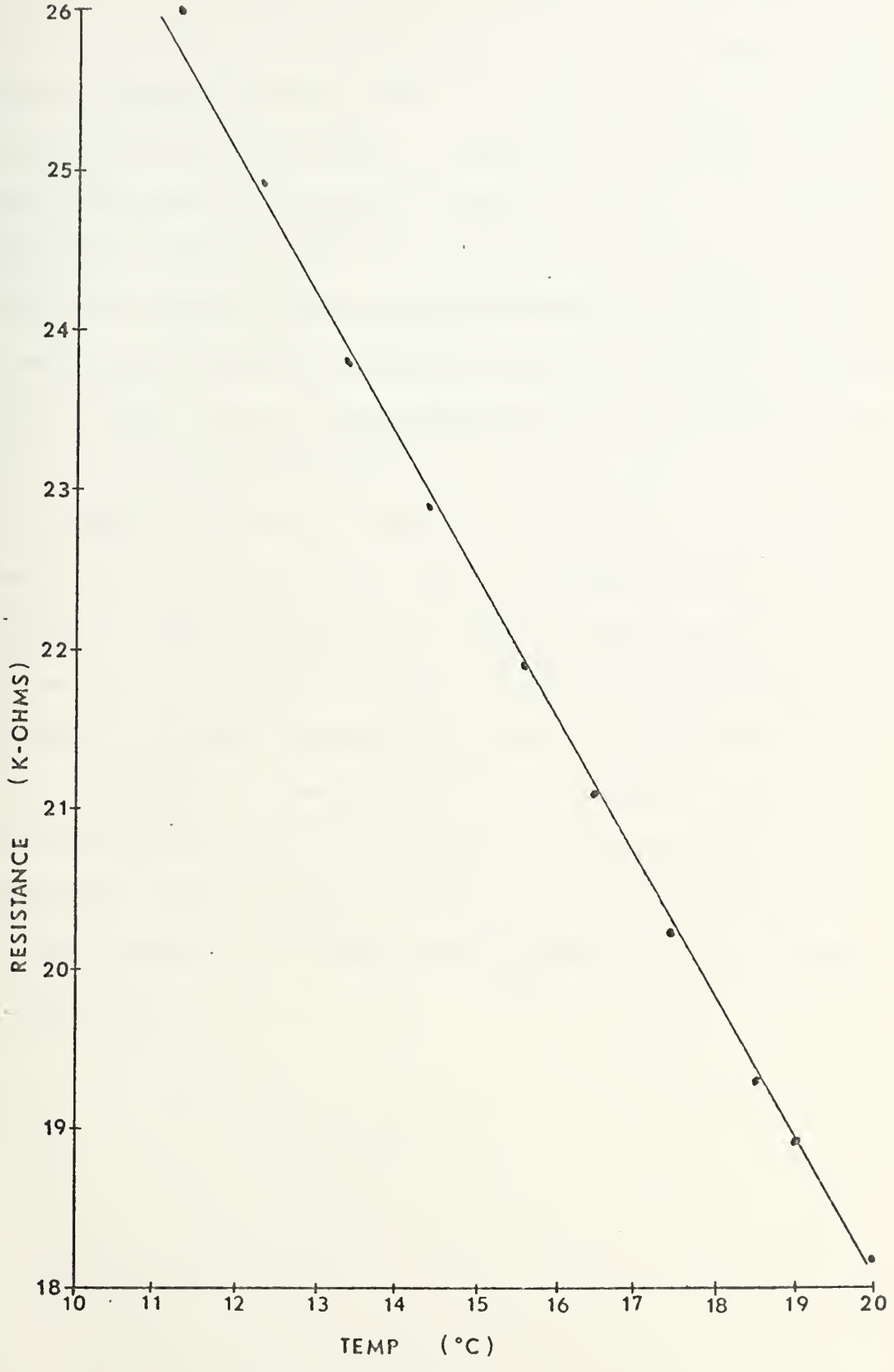

Figure 2. Typical temperature vs resistance calibration curve for Type K496 Thermistors

Each sensor was used as one leg of a Wheatstone bridge (Figure 3). The bridge consisted of two 24.3 K-ohm resistors, the thermistor, and a variable resistor which was used to balance the bridge to zero voltage output at any selected temperature. The output of the bridge was thus a direct measurement of temperature fluctuations about a selected mean. Typical values of bridge output for a selected mean temperature of 18° C were 305 mv per degree C. The advantages of this type of sensor are high sensitivity, high accuracy, interchangeability, fast thermal response time and low cost. The only major disadvantage for oceanographic field work is that they are very fragile.

In addition, wave height, water particle velocity, sound velocity, and salinity were measured. Wave height was measured using the Baylor wave guage which has an accuracy of 1 percent. Water particle velocities were measured on the Engineering Physics Company's Water Current Meter Model EMCM 3B. The time constant of this device is 0.2 seconds and velocity is measured to 1 percent of full scale deflection which for this experiment was 1 cm/sec. These sensors are described in detail by Krapchl [6]. Sound velocity was measured on the Ramsey Corporation Mark I SVTD [Gossner (5)]. Salinity was measured on the Bisset-Berman STD [Frigge (4)].

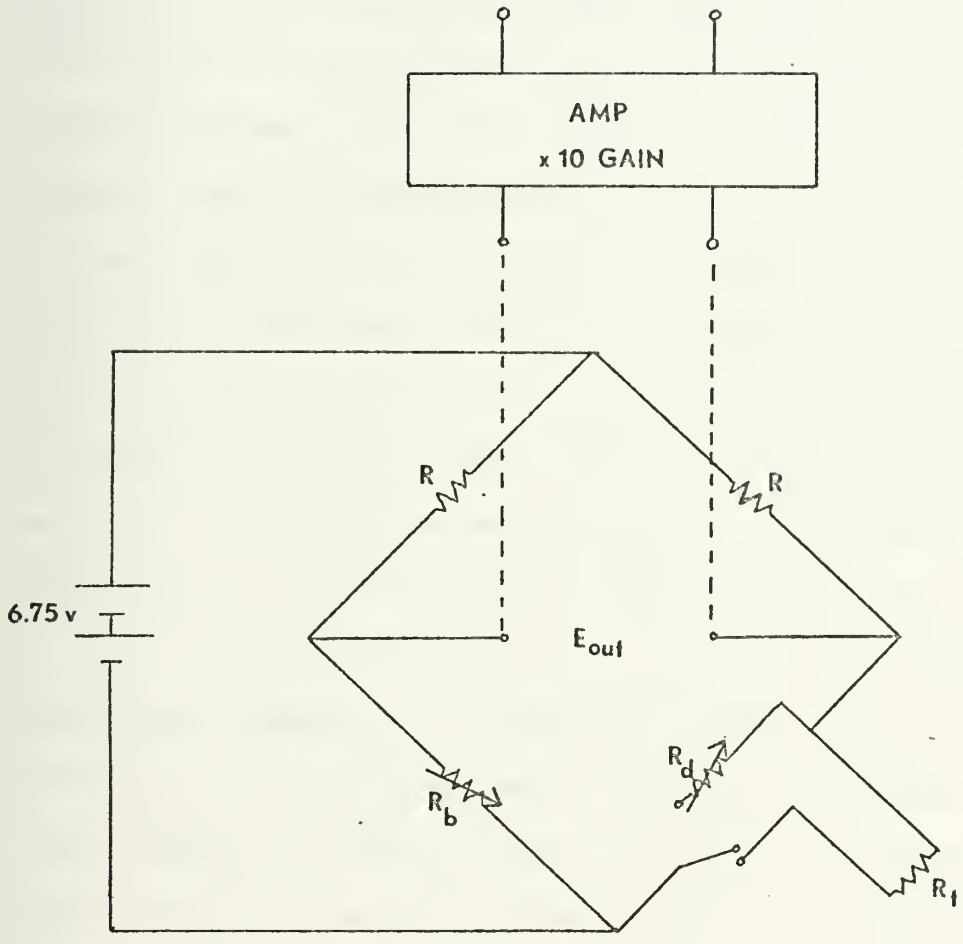

R 24.3 K-OHMS

R_b Balance Resistor

R_d Decade Box

E_{out} Bridge Output

R_t Thermistor

Figure 3. Wheatstone bridge circuit diagram

IV. FIELD EXPERIMENT

The site chosen for conducting this experiment was the Naval Undersea Research and Development Center's Oceanographic Research Tower. The tower is located in 18 meters of water approximately one mile offshore of Mission Beach, San Diego, California. The tower is a steel and concrete structure mounted on four tubular steel legs which are rigidly attached to the bottom. An enclosed upper deck provides adequate space for the installation of a wide variety of electronic equipment and a stable power supply is provided via underwater cable from shore. Rail-mounted carriages are mounted on the north, south, and west sides of the tower and can be moved up and down the sides of the tower with electric winches. Up to 1000 pounds of sensors can be mounted on these carriages and measurements can be made at any desired depth from the surface to one meter above the sea floor.

An instrument mounting frame was constructed to fit the carriages. Sensors were mounted on the frame with consideration given to minimizing interference between sensors while ensuring good coverage of spatial scales expected. Figure (4) shows schematically the positioning of the various sensors. The frame and sensors were mounted on the west side of the tower and were thus open to the full effects of the swell which was propagating from west to east.

Instrumentation wire was led from each sensor to associated electronics in the enclosed upper level. The output of the Wheatstone bridge associated with each temperature sensor was connected to a Preston Model 8300 XWB operational amplifier where a gain factor of ten was applied prior to recording the signal on the Sangamo Model 3562, 14-channel magnetic tape recorder.

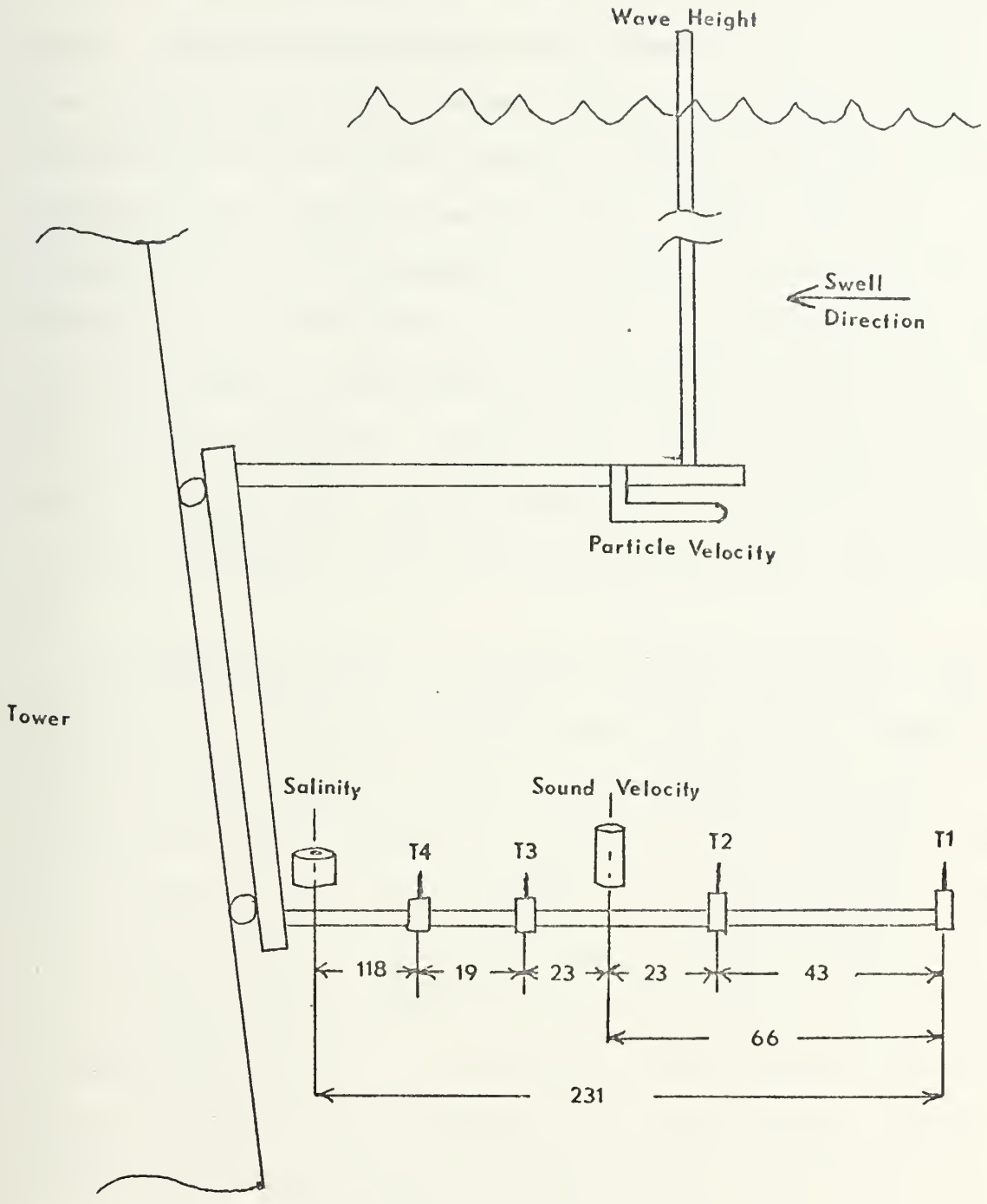

Figure 4. Schematic of sensor placement

On 8 and 9 June, 1972, measurements were made at ten preselected depths. Outputs from each sensor were recorded on eleven of the fourteen available tape recorder channels. Major difficulties were encountered with the temperature sensors. Failure of three of the four available sensors took place early in the experiment. Sensor T4 (Figure 4) failed at the beginning of the first run and sensors T2 and T3 failed early in the second run. In addition, the record from sensor T2 was interupted for approximately one minute in the middle of the first run which effectively removed it from any statistically accurate analysis scheme. Thus no spatial information could be resolved for distances less than 89 centimeters, the distance between sensors T1 and T3.

The thermistor beads of sensors T2, T3 and T4 were found to have sustained major damage and the most probable cause of this damage was contact with the heavy cable of the Baylor wave guage. In normal operation this cable is placed in tension but in order to keep the wave guage centered over the sensor mounting rack it was necessary to attach one end of the cable to the rack and thus the heavy cable had to be raised and lowered by hand through the upper few meters of water prior to tension being applied. It is significant that the only sensor to remain in operation for the duration of the experiment was located farthest from the tower and in a position where it was unlikely to make contact with the wave guage.

V. DATA CONVERSION AND ANALYSIS

The analog data record was played back through a Ci 5000 computer onto an eight channel strip chart recording for editing purposes. Strip chart recordings of each run were first checked for errors that would make them unsuitable for digital analyses. These included such things as short records, clipped signals, and obvious electronic malfunctions. The runs that were not rejected by this procedure were then subjectively analyzed on the basis of environmental parameters, presence or absence of internal wave induced temperature fluctuations, time of data recording and sensor depth. Four runs were subsequently chosen for analysis and are summarized in Table I. The length given for each record is the length of the continuous record used for digital analysis after each signal was edited to ensure that all systems had stablized. Environmental conditions that prevailed during each run are summarized in Table II. In addition to the parameters listed, vertical temperature structure for each run was measured with a mechanical bathythermograph at the start of each run (Figure 5). No values are placed on the temperature axes of this figure as the mechanical BT does not yield accurate absolute temperatures. However it does yield accurate temperature gradient with depth information. The data show that from Run 1 (1405 Local Time) to Run 6 (1922 Local Time) the vertical temperature gradient was reduced to an isothermal condition near the surface. Winds of from 7-10 knots from the southwest were recorded from several hours before Run 1 through Run 5. This wind speed is sufficient to cause some mechanical mixing of the surface waters. Also the air temperature decreased from 67.5° F to 64° F from Run 1 to Run 6. This

TABLE I Summary of Runs Selected for Analysis

Run #	Local Time/Date	Length (Min.)	Depth of Sensors (Ft.)
1	1405/8 June	19.25	18.7
5	1830/8 June	16.67	21.8
6	1922/8 June	17.81	14.3
8	0837/9 June	27.77	14.3

TABLE II Summary of Environmental Conditions for Selected Runs

Run #	Cloud Cover (%)	Wind Dir.	Wind Speed (KTS)	Air Temp. (F)	Sea Sfc. Temp.(F)
1	100	WSW	8	67.5	66.5
5	100	SW	7	64.2	66.0
6	100	SW	4	64.0	65.7
8	100	SW	4	63.1	65.7

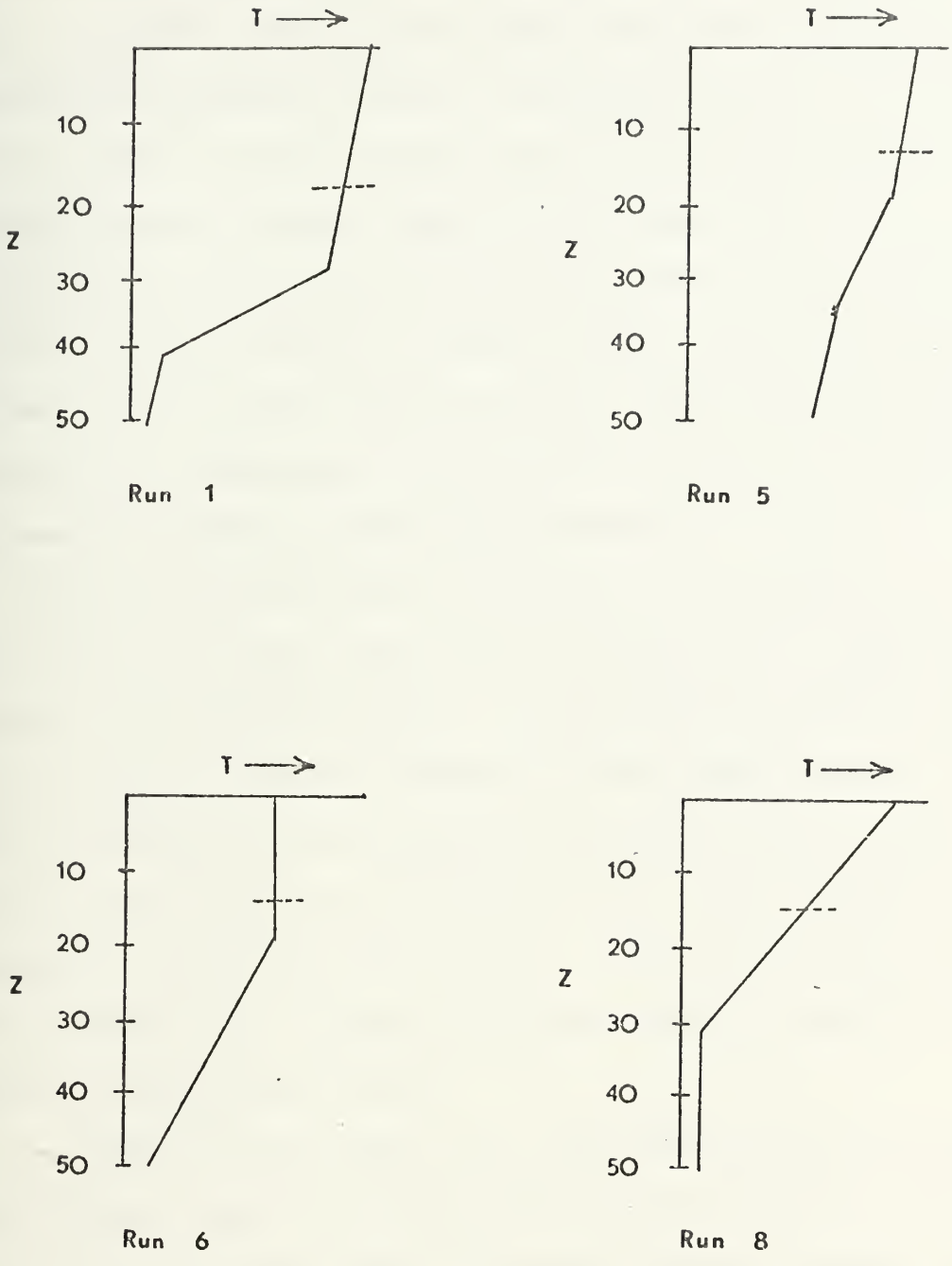

Figure 5. Bathythermographs for selected runs.

(---- indicates sensor depth)

decrease was accompanied by a decrease in sea surface temperature from 66.5° F to 65.7° F. This surface water cooling would be expected to be accompanied by convective overturn and therefore mixing of the surface waters. Either of these processes would give rise to the observed vertical thermal structure changes and most likely both were at work. Both processes are non-linear, turbulent processes. From the beginning of Run 6 till the end of Run 8 winds were calm. The increased near-surface vertical thermal gradient observed in Run 8 is probably due to warming of the surface waters by the early morning sun, although the sky remained overcast throughout the experiment.

Each of the runs selected for analysis were digitized by inputing the analog record into a hybrid system consisting of a Ci 5000 analog computer and a XDS 9300 computer. A standard analog to digital conversion program was used to generate a 7-track digital magnetic tape. Since a great deal of core space was required for digital analysis of the data the 7-track tape was converted to a 9-track tape which was compatible with the IBM 360/67 computer. Conversion was executed on the IBM 360/67 using a standard conversion program. Analysis of each selected run was then performed.

For each pair of variables (e.g., temperature and sound velocity fluctuations), means and variances were calculated and the means were subtracted. Any linear trends were removed and auto-covariance and cross-covariance functions were calculated. A Parzen window was applied to the covariance functions to account for the finite length of records. The spectral energy density spectra and the cross-spectral energy density spectrum were calculated by Fourier transforming the auto- and cross-covariance functions. The phase and coherence-functions were calculated

using the cross-spectral quantities. Graphs of the auto-correlation, cross-correlation, spectral energy density, coherence, and phase functions were plotted using the Cal-comp plotter.

VI. DISCUSSION OF RESULTS

A. SURFACE WAVE INDUCED TEMPERATURE FLUCTUATIONS

Figure (6) is a plot of energy density spectra, coherence and phase for temperature and wave height for Run 6. Maximum energy of the temperature spectrum is centered at the frequency of maximum surface wave energy (.064 Hz) which corresponds to a wave period of approximately 15.6 seconds. Maximum coherence (.68) is found at this frequency and relative maxima in coherence generally occur at frequencies corresponding to those of relative maxima in the wave spectrum. The phase relationship is relatively constant in the range from about .03 Hz to .2 Hz at a value of 180^{o}. The waves in this frequency band were swell type waves. The high coherence values at frequencies of relative maxima in the wave spectrum and the 180^{o} phase difference in the swell frequency band apparently verify the assumed relationship between surface swell and temperature fluctuations. The coherence and phase relationships between temperature fluctuations and water particle velocity components further verify the temperature/wave relationship. Linear theory predicts that the horizontal components of wave-induced water particle velocity should be in phase with wave height fluctuations and that the vertical velocity component should be 90^{o} out of phase. As previously stated, Kraphol [6] showed that the waves associated with this experiment were highly linear. The phase relations outlined above should hold between temperature fluctuations and the velocity components. Figures 7 and 8 are plots of spectra, coherence, and phase for T vs u and T vs w respectively. T vs u displays relatively high coherence (.61) at the frequency of maximum wave energy with a phase angle of 180^{o}. T vs w displays high coherence at the same frequency but with a phase angle of 90^{o} from .03 Hz to .22 Hz.

Figure 6.
Spectra, coherence, and phase
for temperature and wave height,
Run 6

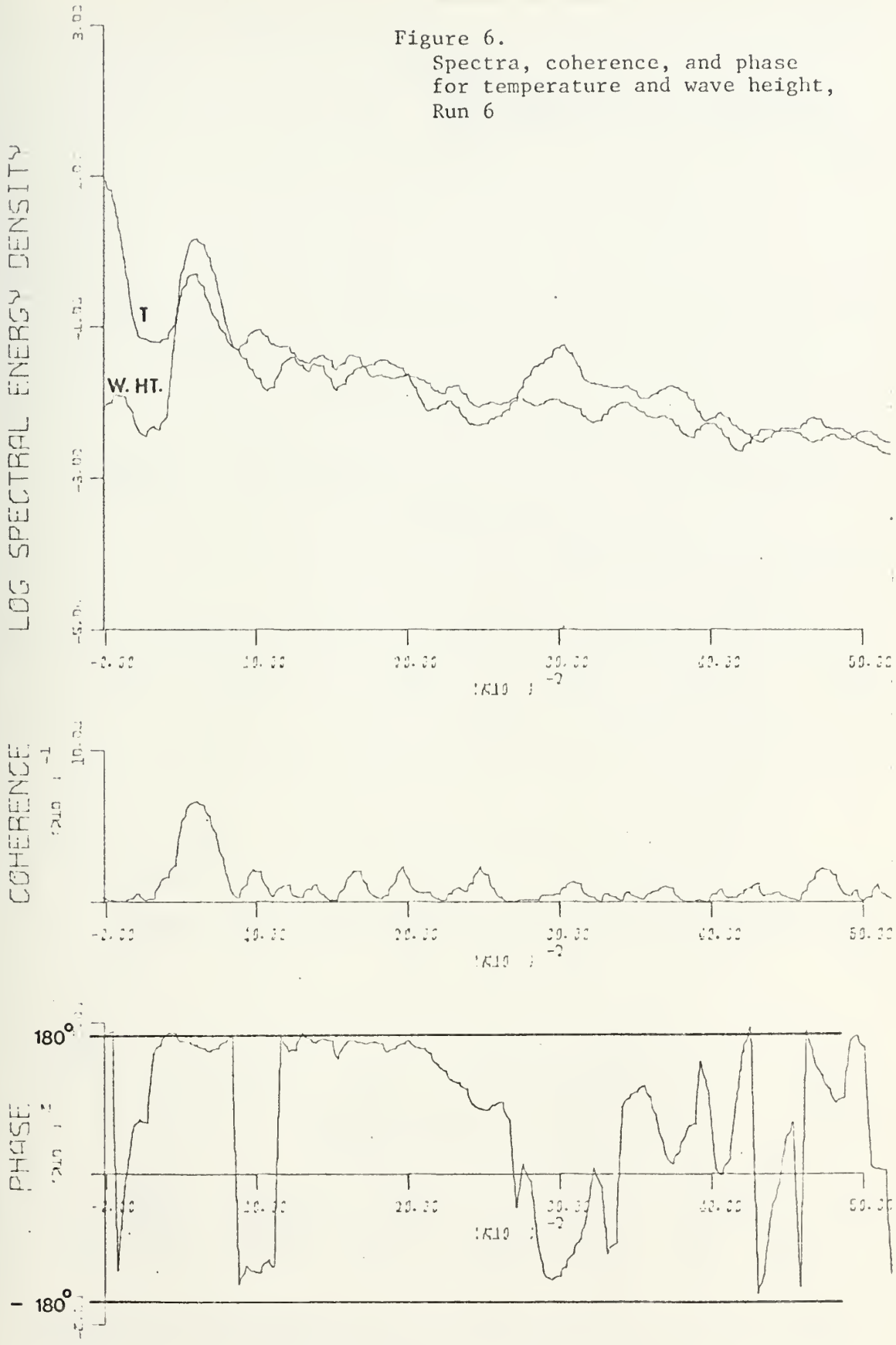

Figure 7.
Spectra, coherence, and phase
for temperature and u-component,
Run 6

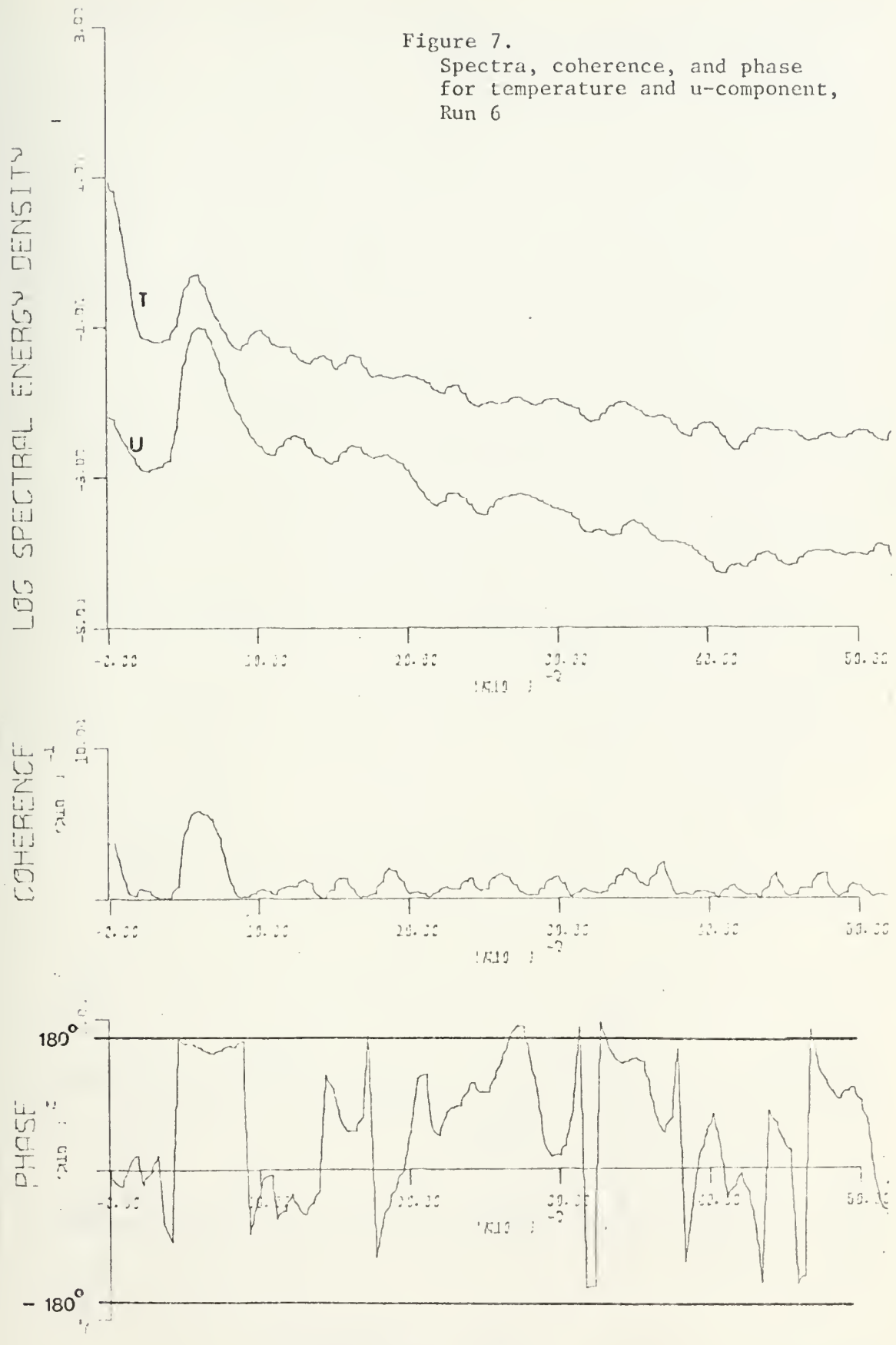

Figure 8.
Spectra, coherence, and phase
for temperature and w-component,
Run 6

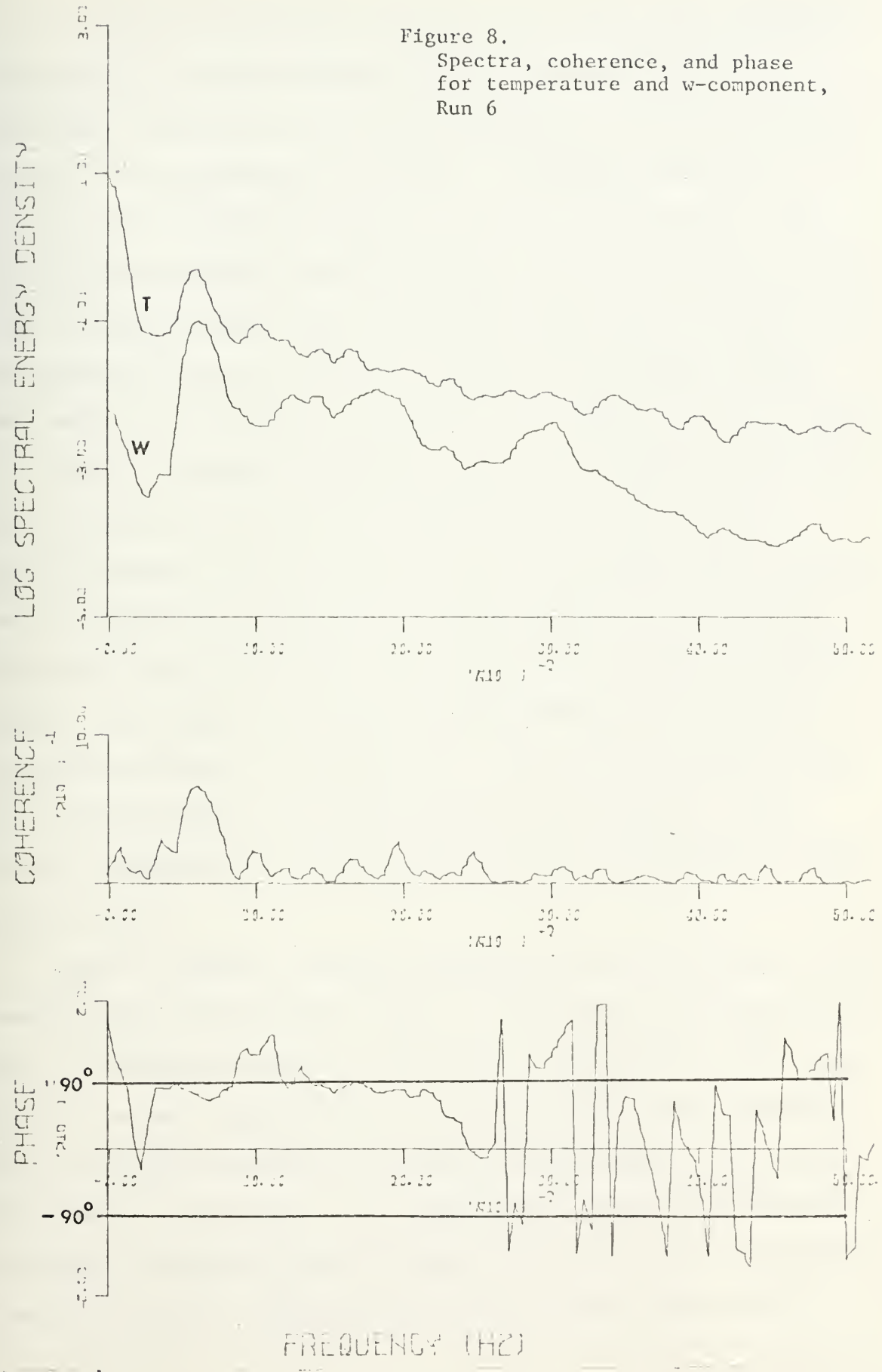

An anomaly in this pattern exists at about .1 Hz. This frequency corresponds to a relative maximum in the energy density spectrum of temperature fluctuations and a relative minimum in the spectra of wave height, u- and w-components of velocity. A coherence maximum (.2) occurs at this frequency for both T vs w and T vs wave height. The phase between temperature and wave height is -120^{o} which does not agree with the predicted phase angle. The phase angle between temperature and w-component of velocity is 150^{o} and thus the 90^{o} phase angle between wave height and w-component of velocity is as predicted by linear theory.

Figures 9 through 17 are similar plots for temperature, wave height, and water particle velocities for Runs 5, 1 and 8. All runs are in general agreement with the results of Run 6. Run 5 has almost identical results, displaying slightly lower coherence values at the frequency of maximum energy and slightly less consistency in the phase relationships. These results still show very good adherence to the assumed temperature-surface wave relationship. Runs 1 and 8 show significantly lower coherence values and more random phase relationships. These results, though less striking, are still in general agreement with those of Runs 5 and 6.

Figure 5 provides a possible explanation for the differences observed between Runs 5 and 6 and Runs 1 and 8. It was shown in equation (II-14) that in the frequency band of surface swell, the coherence between temperature and wave height will be strictly less than one if temperature fluctuations are assumed to be composed of wave induced and turbulent fluctuations. Furthermore it was shown that as turbulent fluctuations increased, the coherence would decrease. Since the swell waves present remained relatively constant for all runs, we would expect that at

Figure 9.
Spectra, coherence, and phase
for temperature and wave height,
Run 5

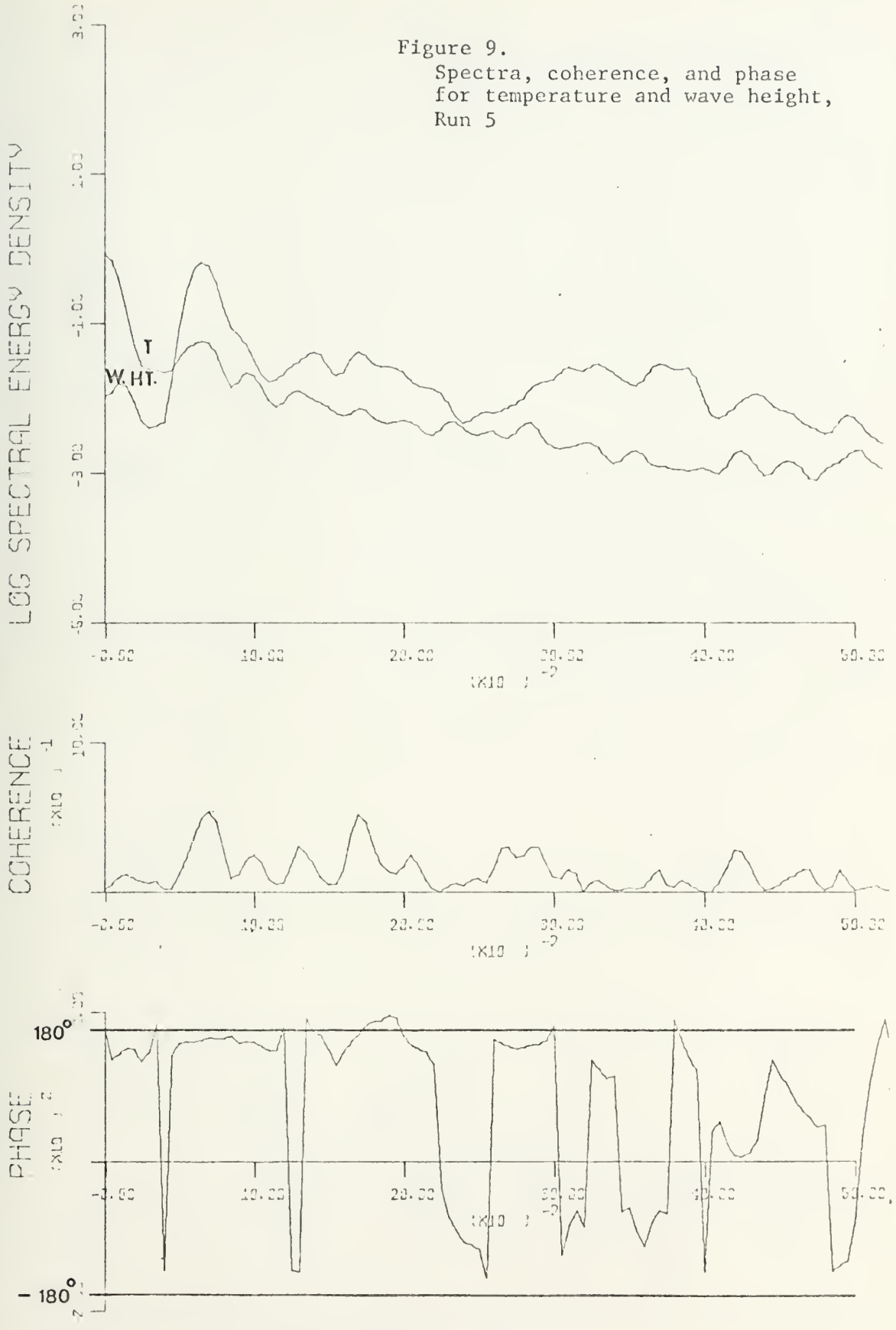

Figure 10.
Spectra, coherence, and phase
for temperature and u-component,
Run 5

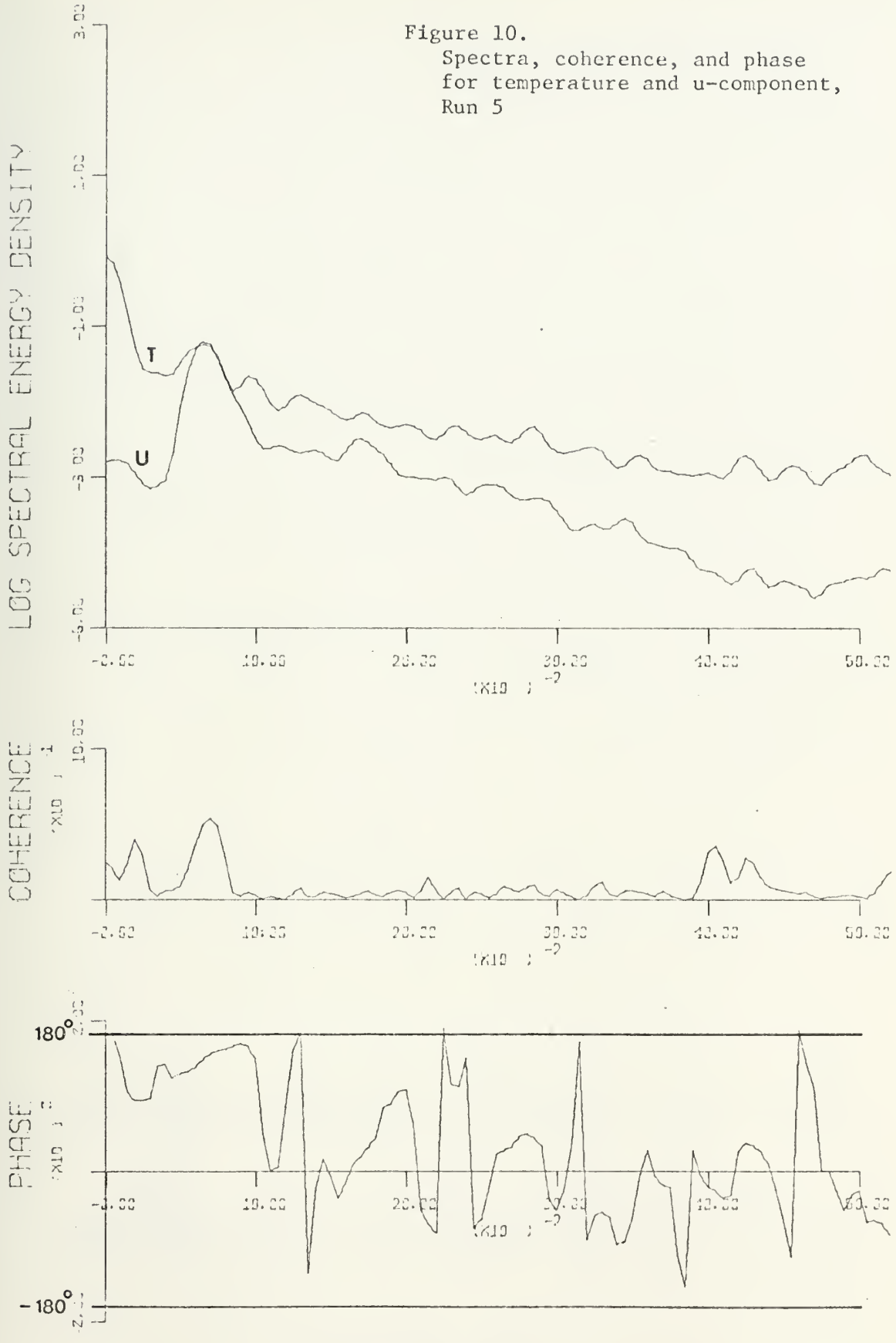

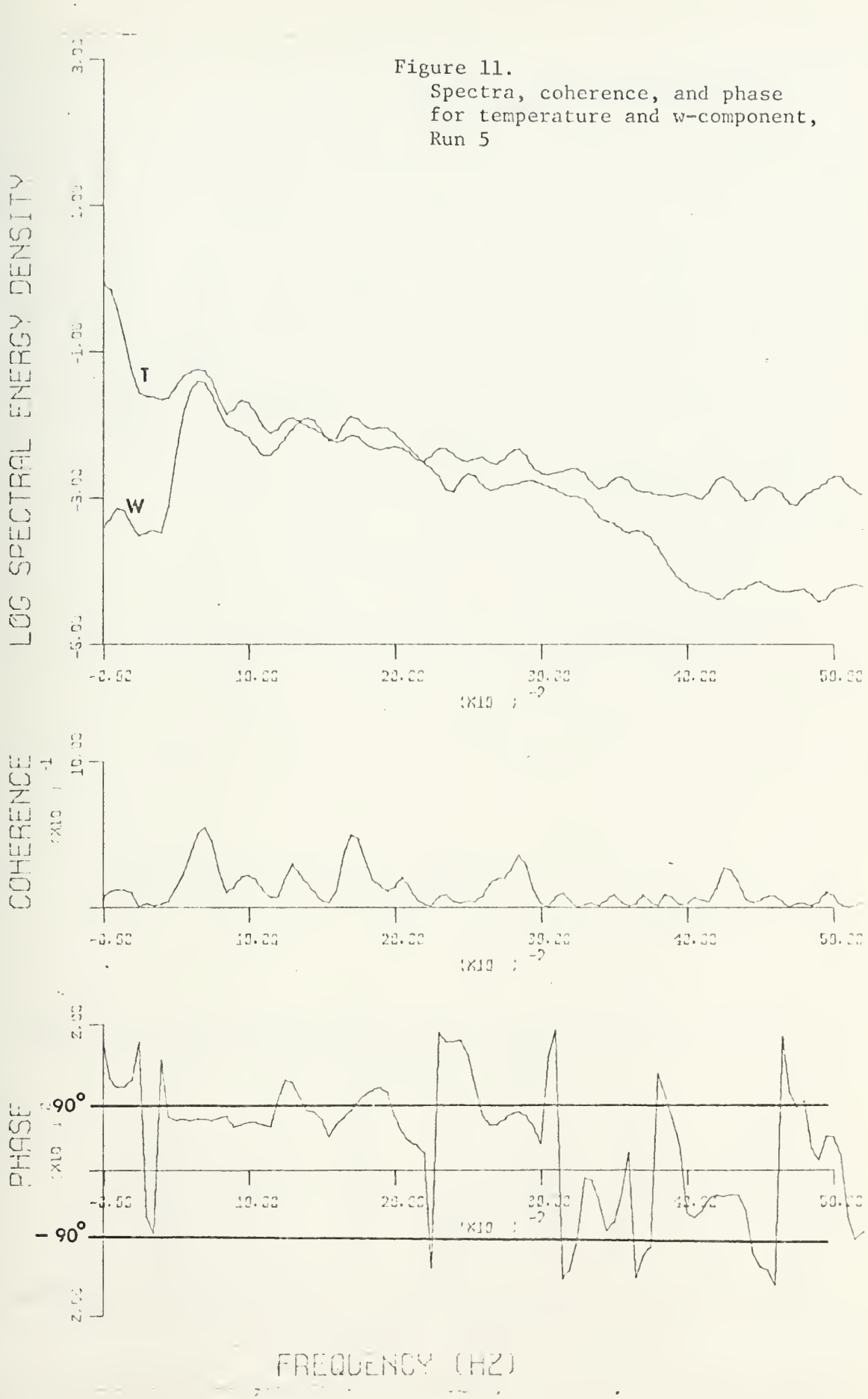

Figure 11.
Spectra, coherence, and phase for temperature and w-component, Run 5

Figure 12.
Spectra, coherence, and phase for temperature and wave height, Run 1

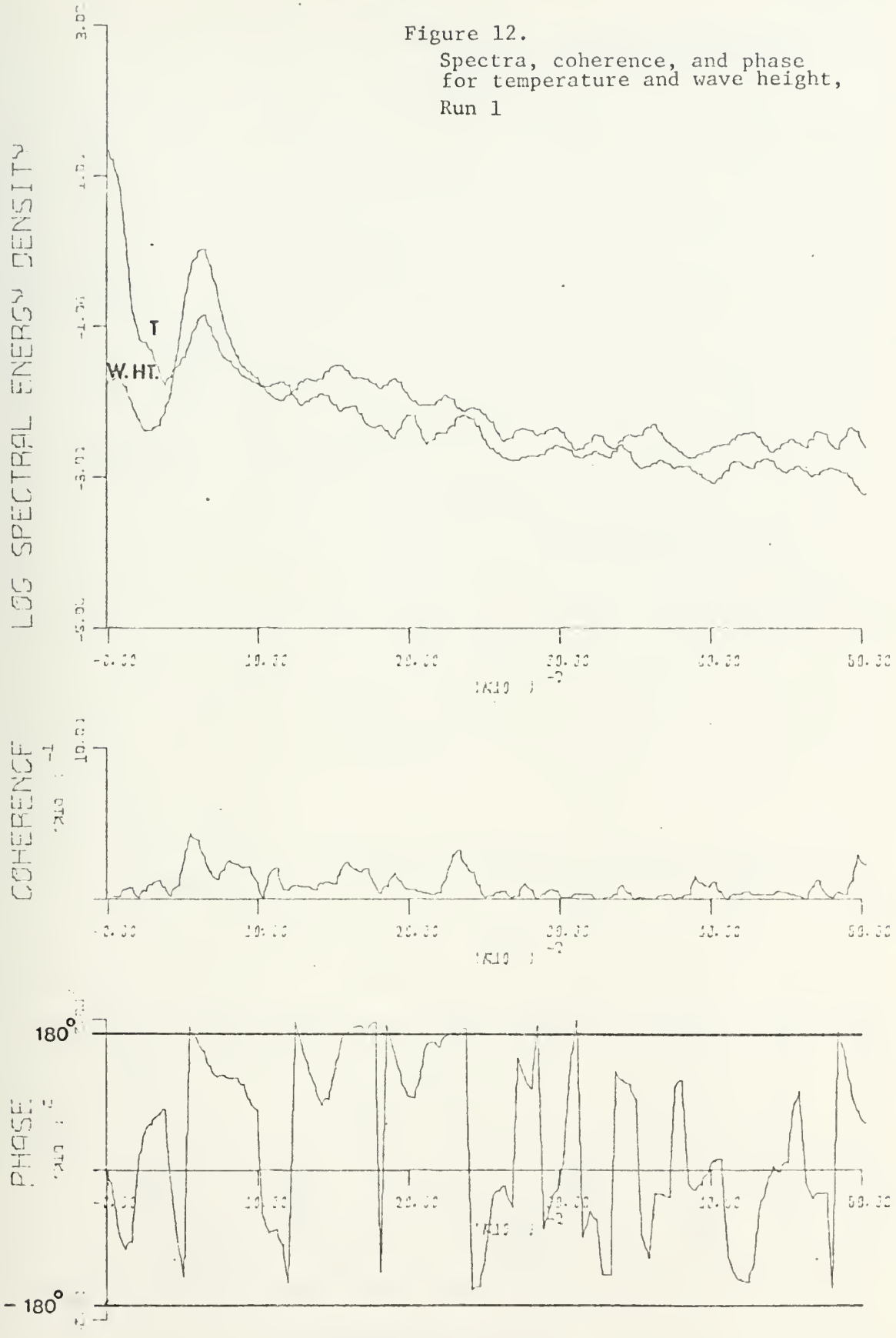

Figure 13.
Spectra, coherence, and phase
for temperature and u-component,
Run 1

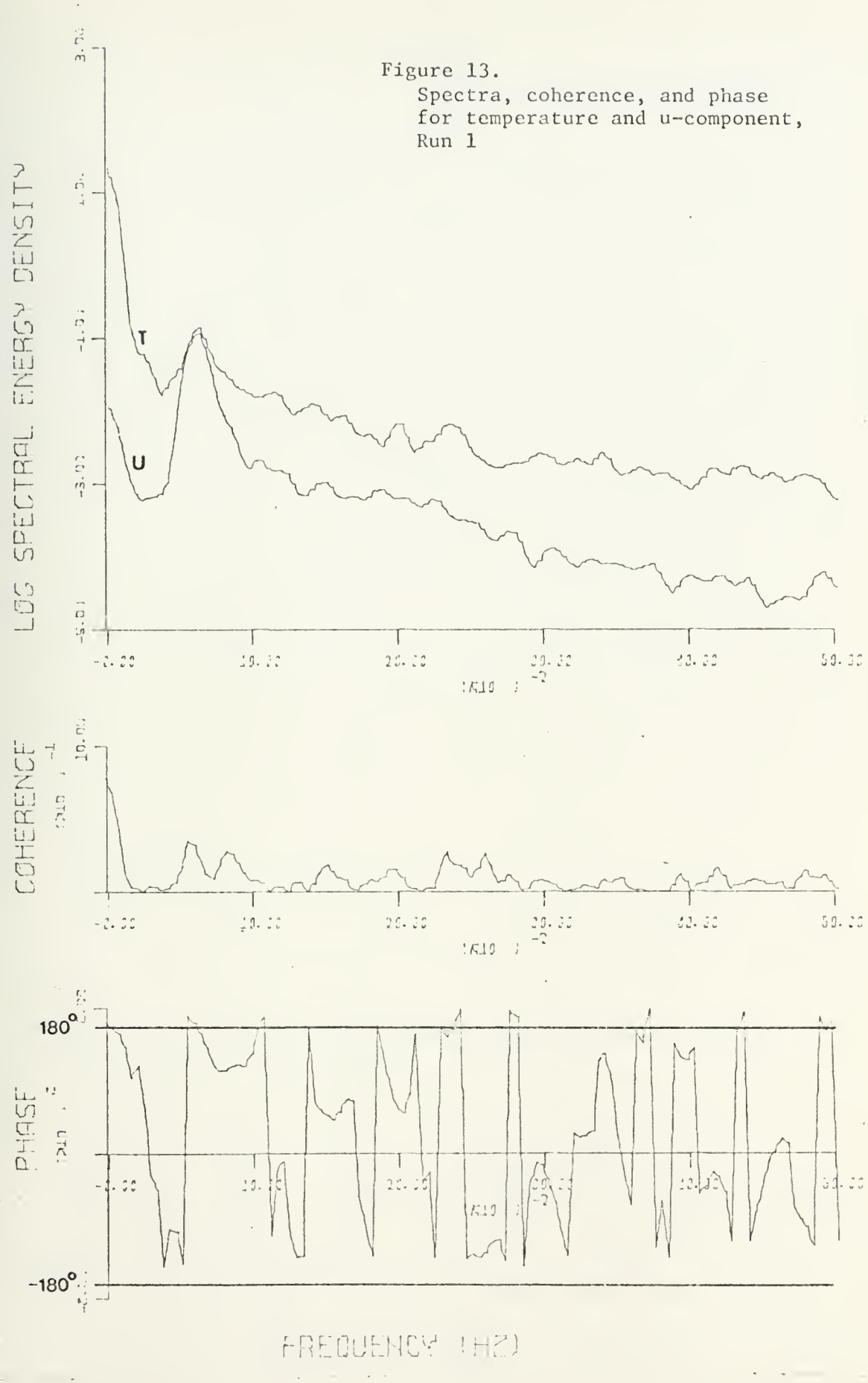

Figure 14.
Spectra, coherence, and phase
for temperature and v-component,
Run 1

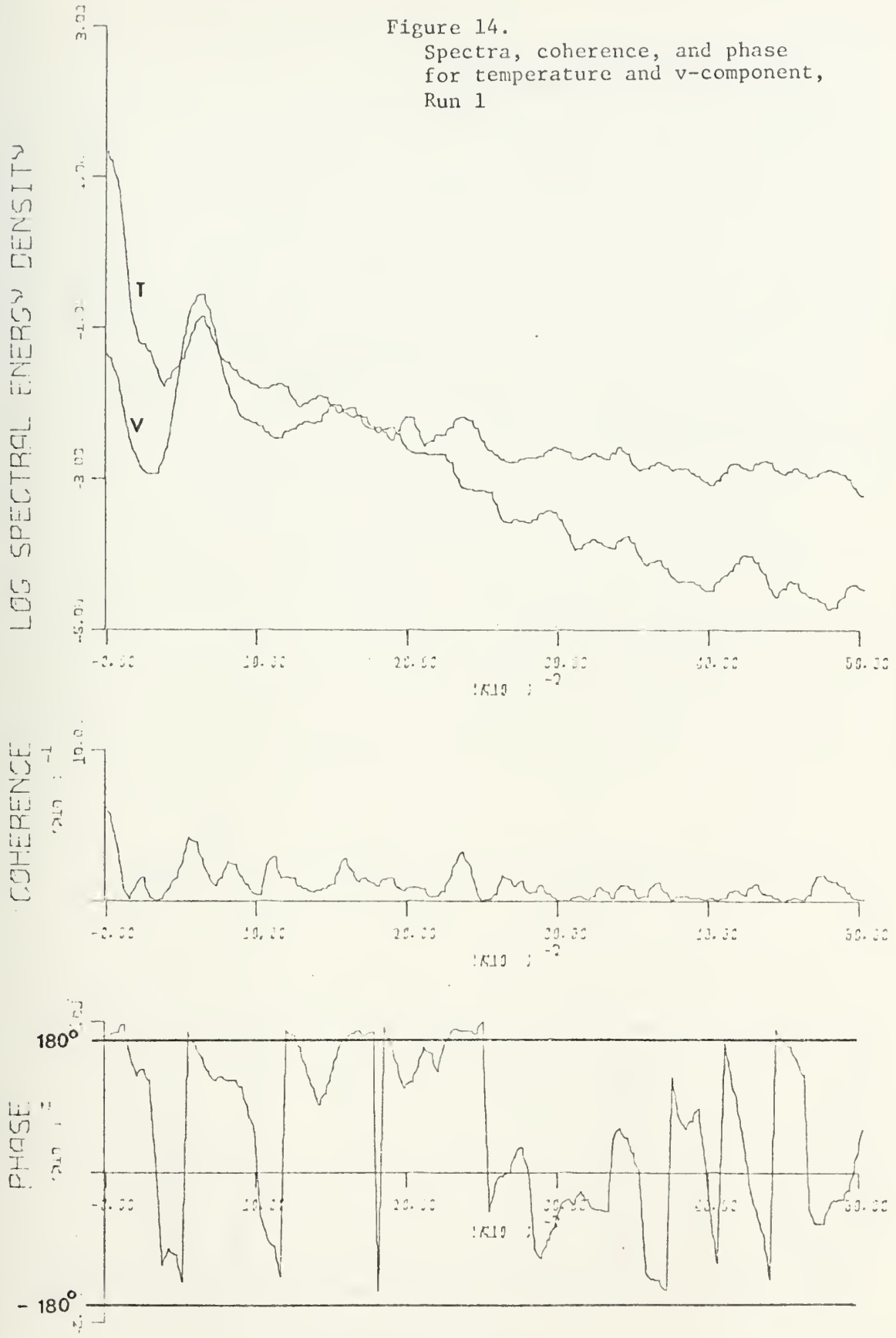

Figure 15.
Spectra, coherence, and phase
for temperature and wave height,
Run 8

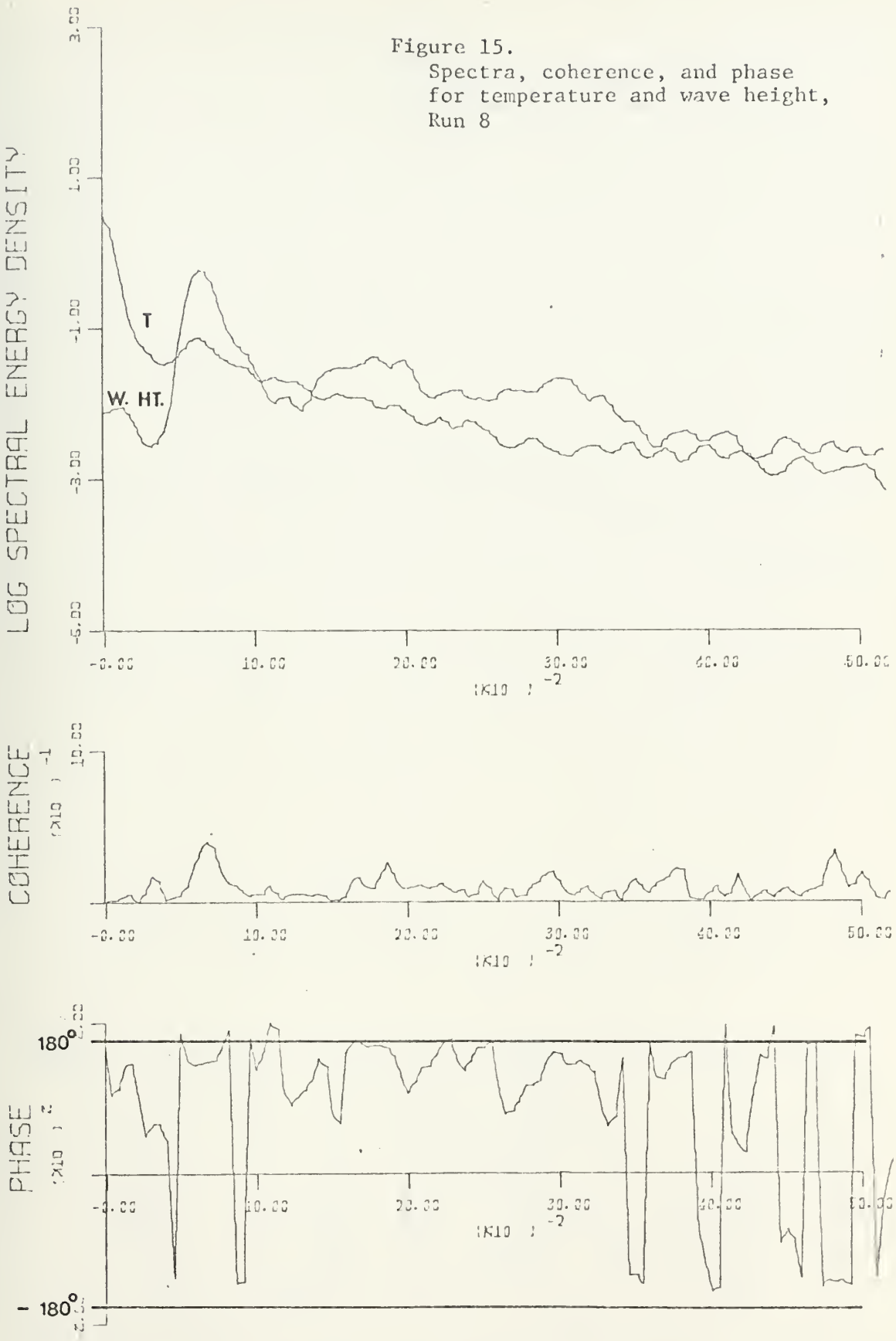

Figure 16.
Spectra, coherence, and phase
for temperature and u-component,
Run 8

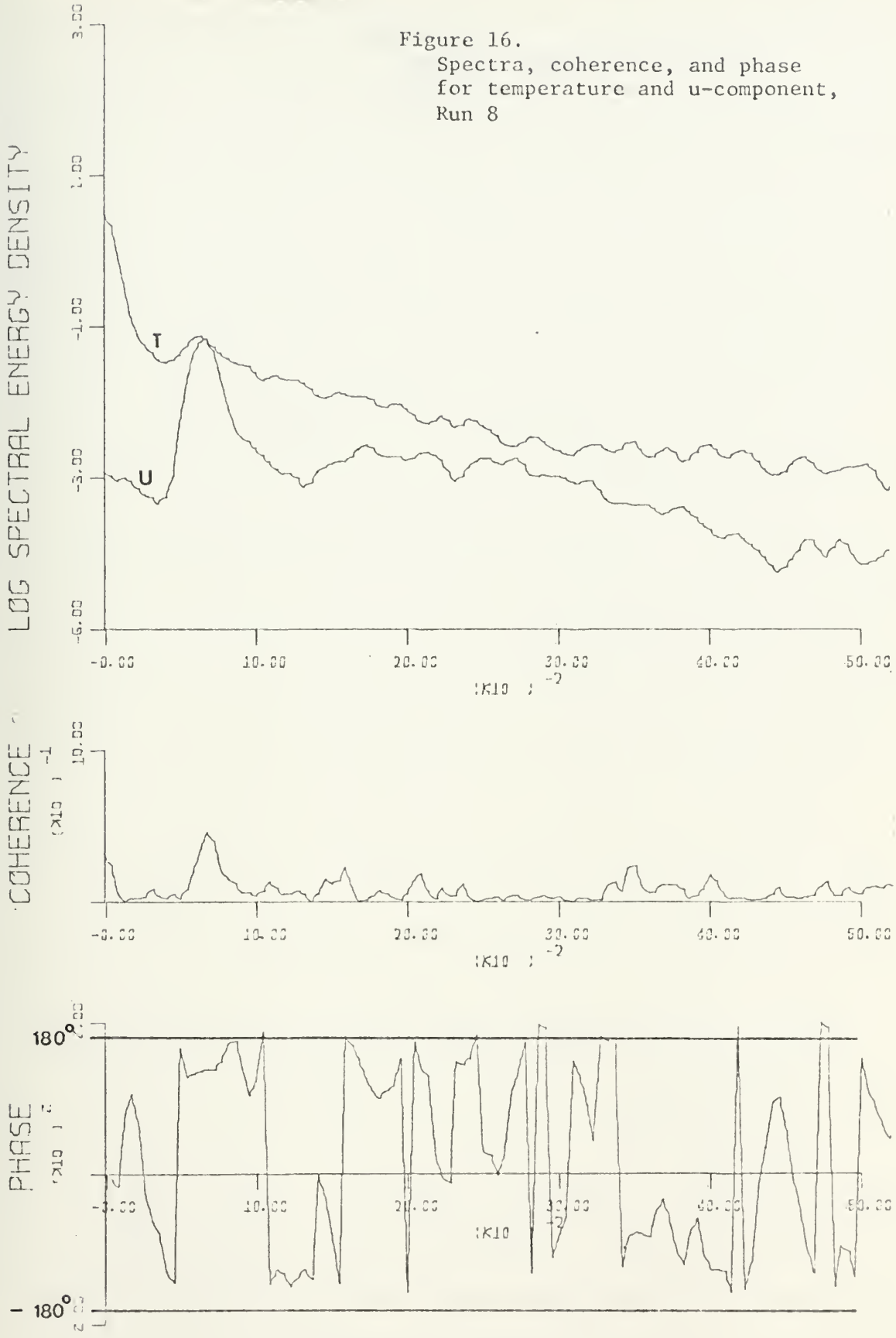

Figure 17.
Spectra, coherence, and phase
for temperature and v-component,
Run 8

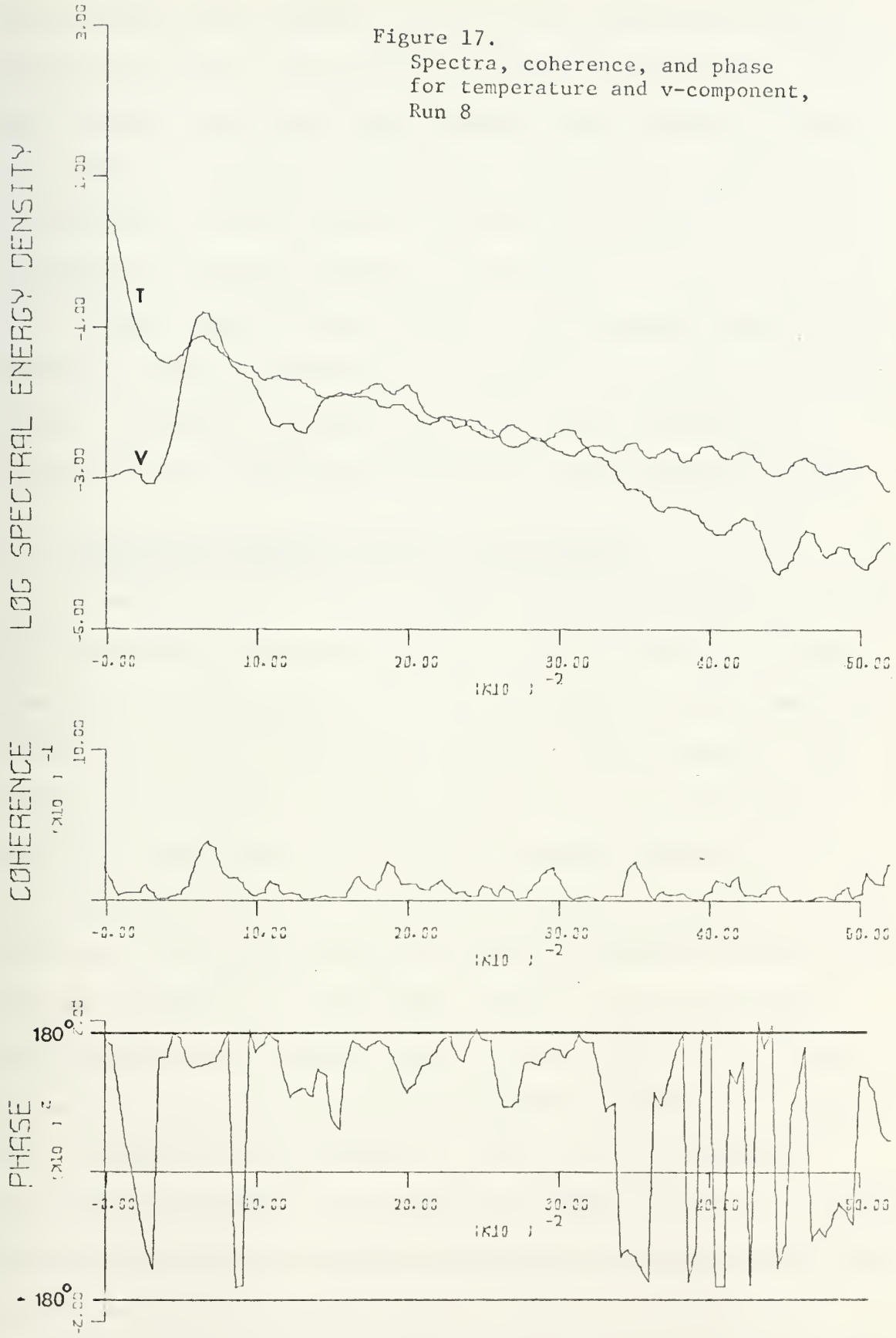

constant depth, the turbulent velocity field strength would remain relatively constant in the frequency band under consideration. Since Run 6 and Run 8 were made at the same depth, the differences between them cannot be attributed to changes in the turbulent velocity field. In the absence of a well defined temperature gradient (Runs 5 and 6) we would expect turbulent temperature fluctuations to be quite small; and with a larger gradient (Runs 1 and 8), we would expect higher levels of turbulent temperature fluctuations regardless of the turbulent velocity field. For example, we would observe no turbulent temperature fluctuations in a turbulently well mixed, constant temperature bath.

B. INTERNAL WAVE INDUCED TEMPERATURE FLUCTUATIONS

Inspection of strip chart recordings showed that Run 1 was the only run selected for analysis that contained any significant long period components. The temperature signal from thermistor T1 was summed and averaged for each 12 second interval for all records analyzed. The results of the averaged temperature signal for Run 1 are plotted in Figure 18. Only three long term fluctuations were observed. The fluctuations displayed a 6 to 9 minute period and were quasi-cycloidal in shape. The average temperature change from maximum temperature to minimum temperature was approximately $.48^{\circ}$ C. If the temperature fluctuations due to internal waves do in fact reflect the vertical movement of the vertical temperature gradient, [Equation I-1], then with a measured thermal gradient of $.008^{\circ}$ C/cm, this temperature fluctuation corresponds to an internal wave height of 60 cm. It should be noted that negative temperature fluctuations indicate positive wave heights and vice-versa if the assumed internal wave-temperature relationship is correct. The phase difference with a negative gradient

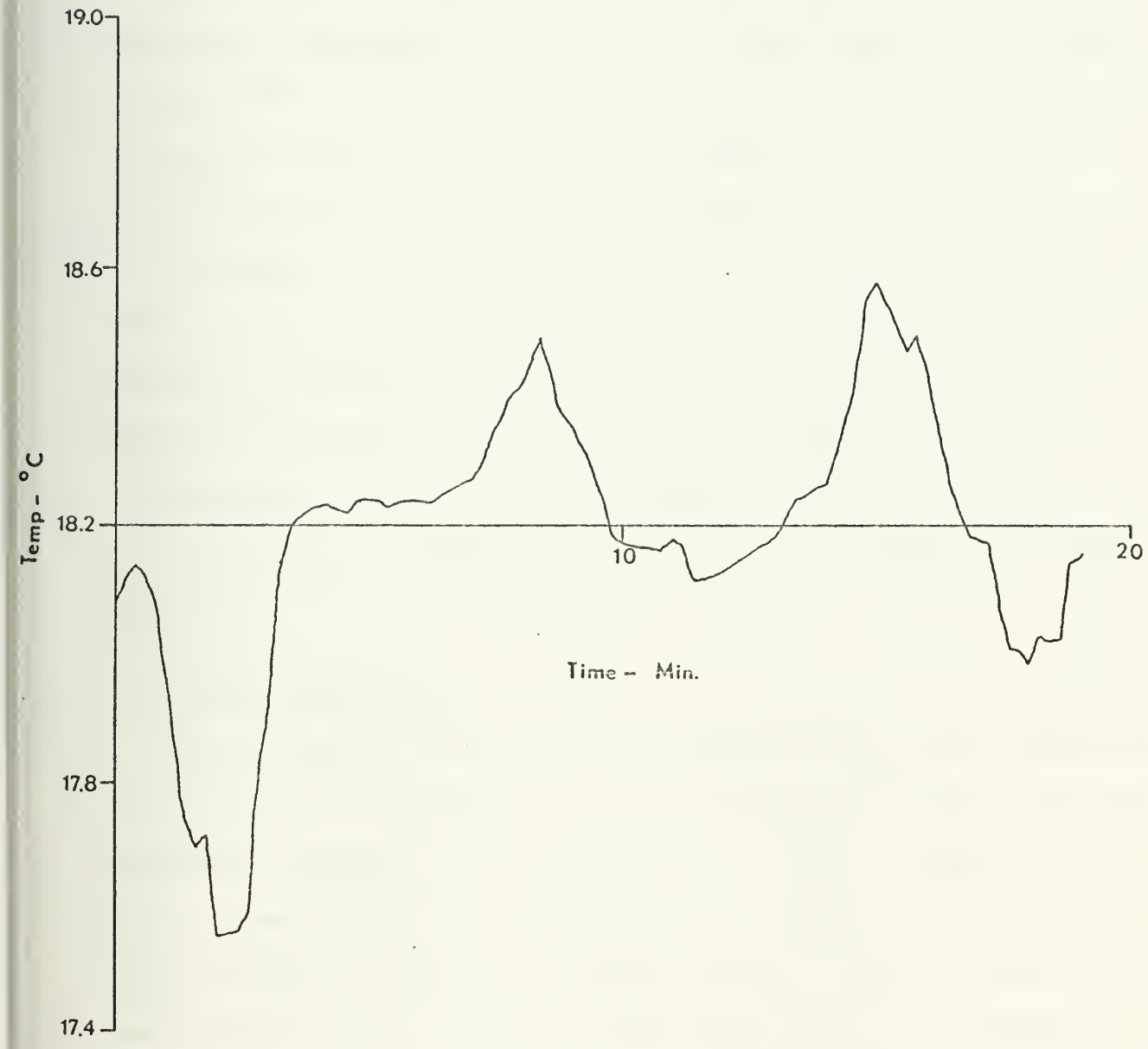

Figure 18. Temperature averaged each 12 seconds for Run 1

should be 180°. Figure 19 is a plot of the v-velocity component averaged each 12 seconds in the same way as the average temperature plot. On this, the average temperature fluctuation has been superimposed and the phase reversed 180°. The same internal wave can be seen to manifest itself in the water particle velocity record. Referring to Figures 6 through 17, it can be seen that for Run 1 the coherence values at low frequencies are very high for T vs u (.72) and T vs v (.62) and the phase angle is 180°. For Runs 5, 6 and 8, which had little internal wave activity, coherence values are quite low at low frequencies. Figures 20 and 21 are plots of spectra, coherence and phase for sensor T3 and the u- and v-components of velocity for Run 1. Values of coherence and phase at low frequencies are observed to be similar to those obtained from sensor T1.

C. SPATIAL RELATIONSHIPS

Due to breakage of thermistors and technical problems with electronics, only Run 1 has a record where more than one temperature sensor functioned. Temperature sensors T1 and T3 (Figure 4) functioned throughout Run 1. The distance between these sensors was 89 cm. Figure 22 is a plot of the auto-correlation functions for sensors T1 and T3. They are quite similar out to about a lag of 22 seconds, after which, there is a difference between them of 2% and more, but they are in general agreement. Figure 23 is a plot of the cross-correlation between T1 and T3. It has a maximum value of .95 at a lag time of 14 seconds. Thus T1 and T3 are most highly correlated when lagged 14 seconds. Figure 24 is a plot of the spectra, coherence and phase of T1 and T3. The highest coherence value (.93) is found in the low frequencies. The 14 second lag for a maximum cross-correlation value is thus probably associated with internal waves. If

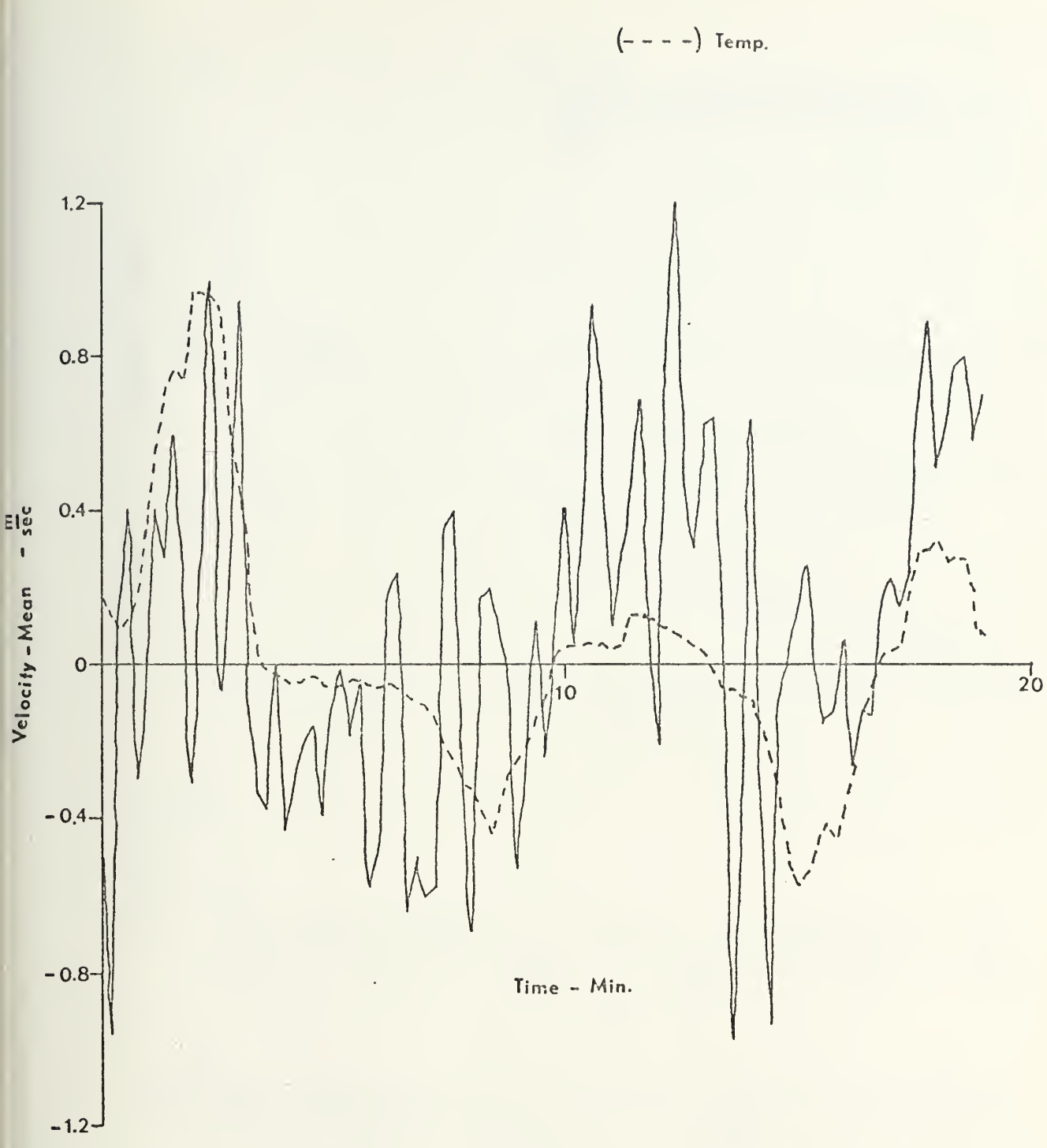

Figure 19. V-component of velocity averaged each 12 seconds with averaged temperature signal superimposed and shifted 180°.

Figure 20.
Spectra, coherence, and phase
for temperature (T3) and v-component,
Run 1

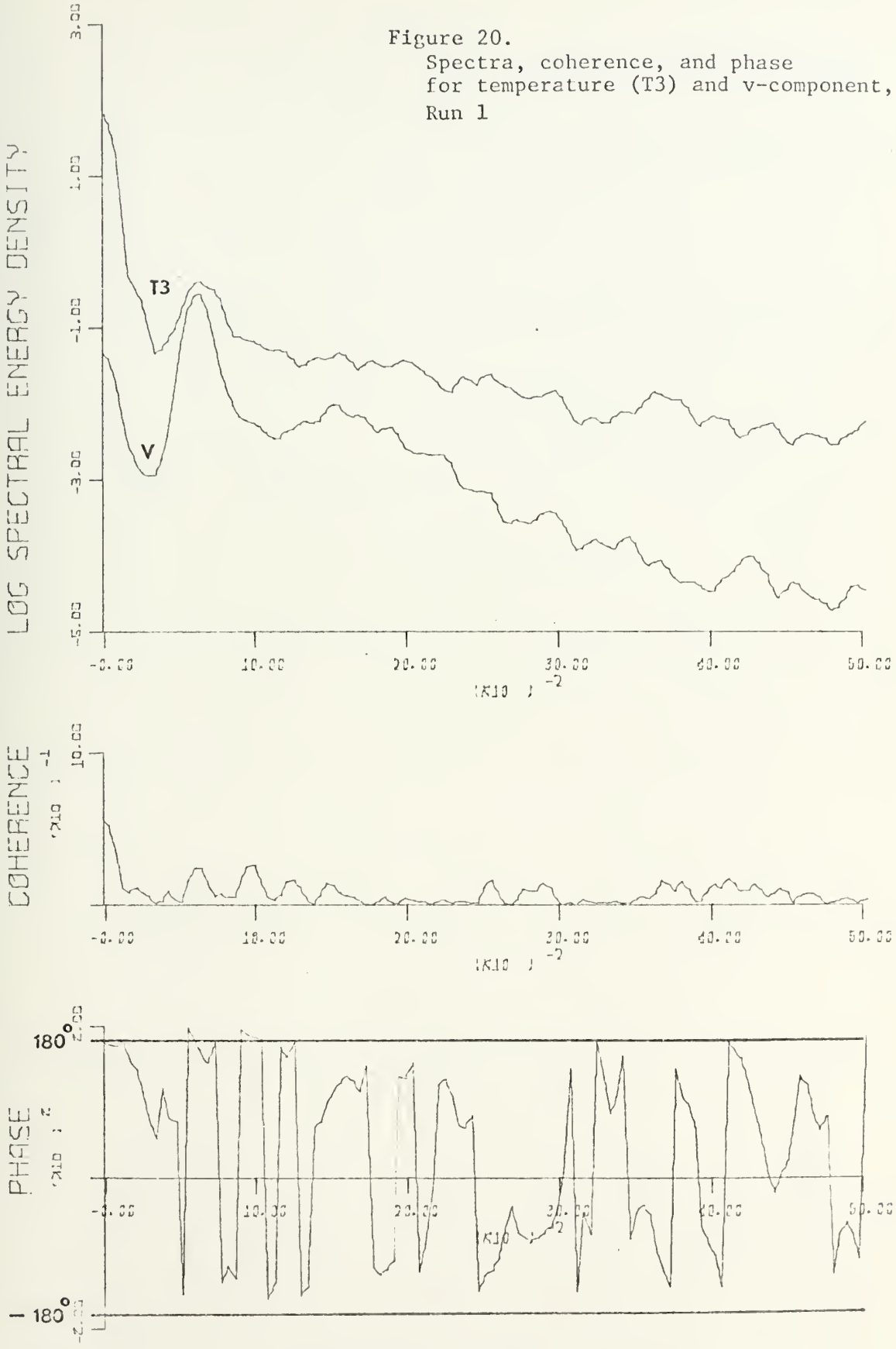

Figure 21.
Spectra, coherence, and phase
for temperature (T3) and u-component,
Run 1

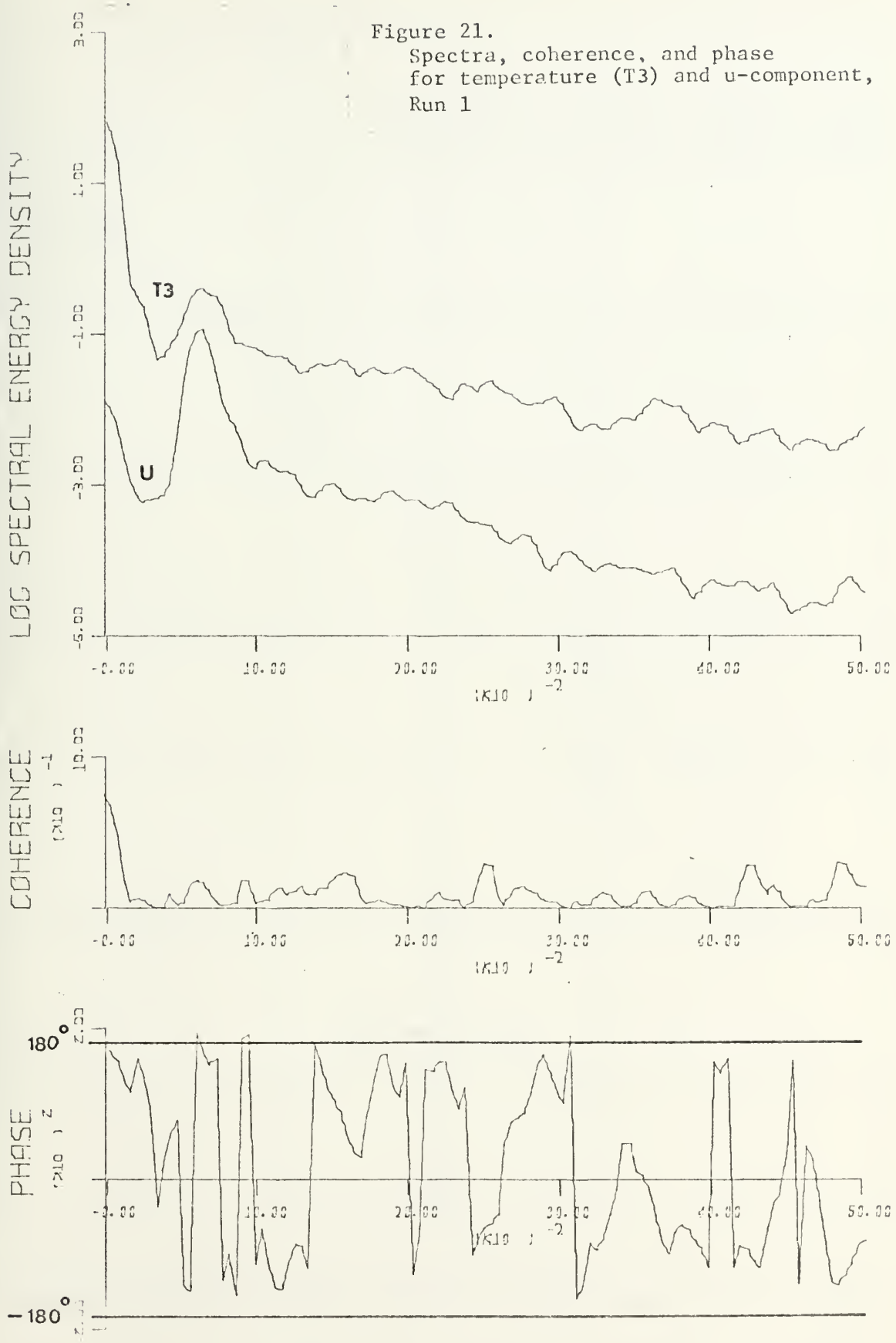

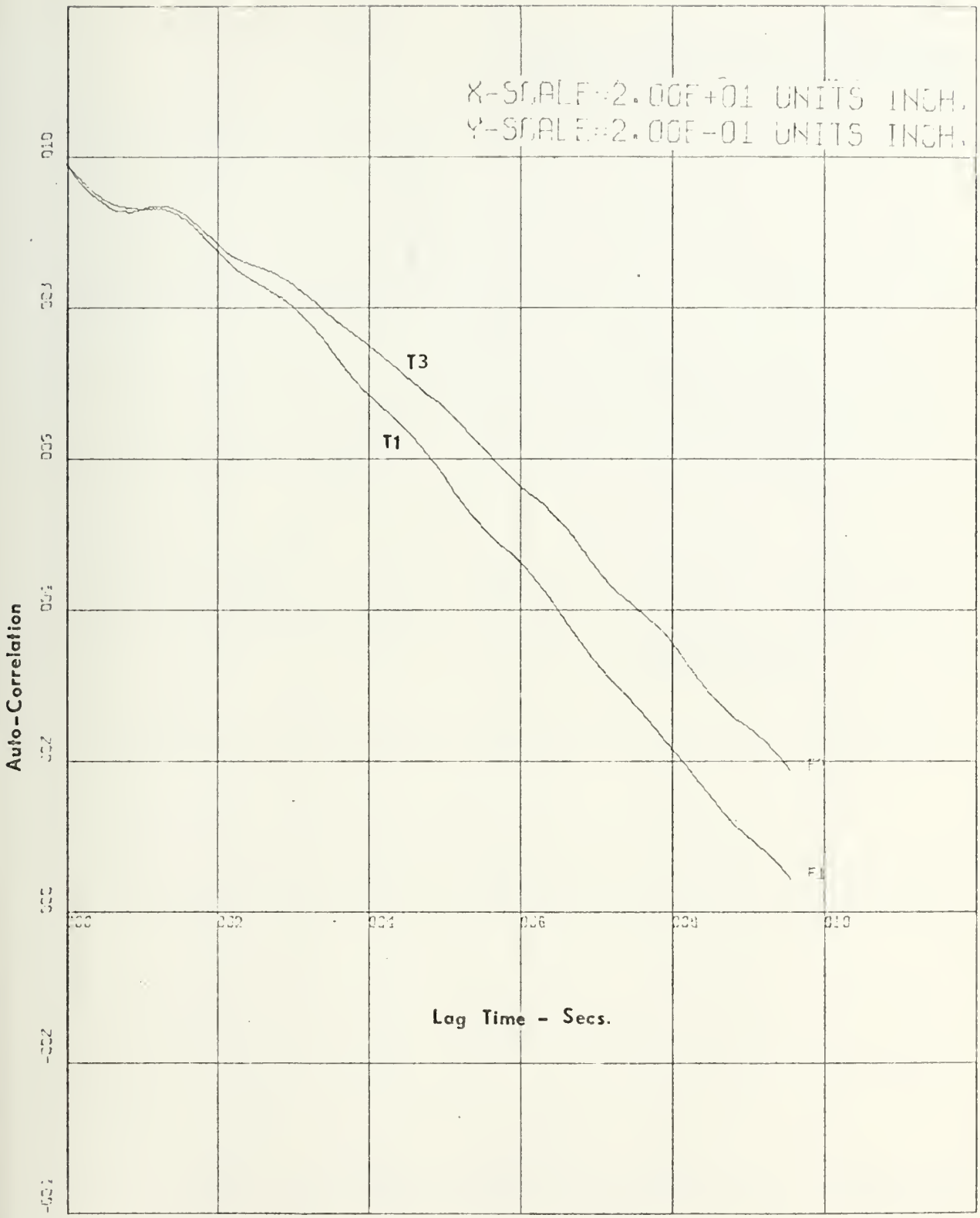

Figure 22. Auto-correlation functions for thermistors T1 and T3, Run 1

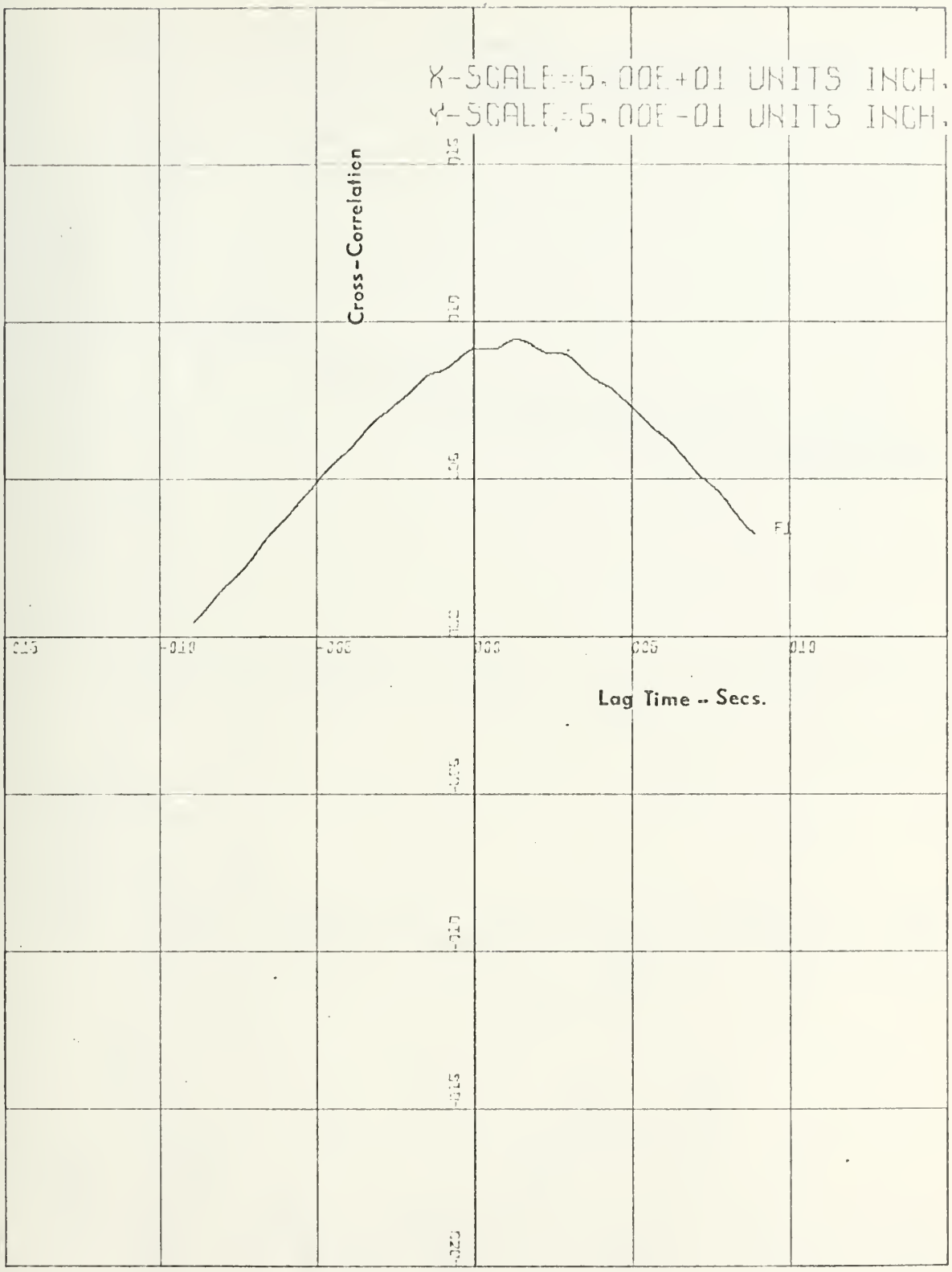

Figure 23. Cross-correlation function for thermistors T1 and T3, Run 1

Figure 24.
Spectra, coherence, and phase
for thermistors T1 and T3,
Run 1

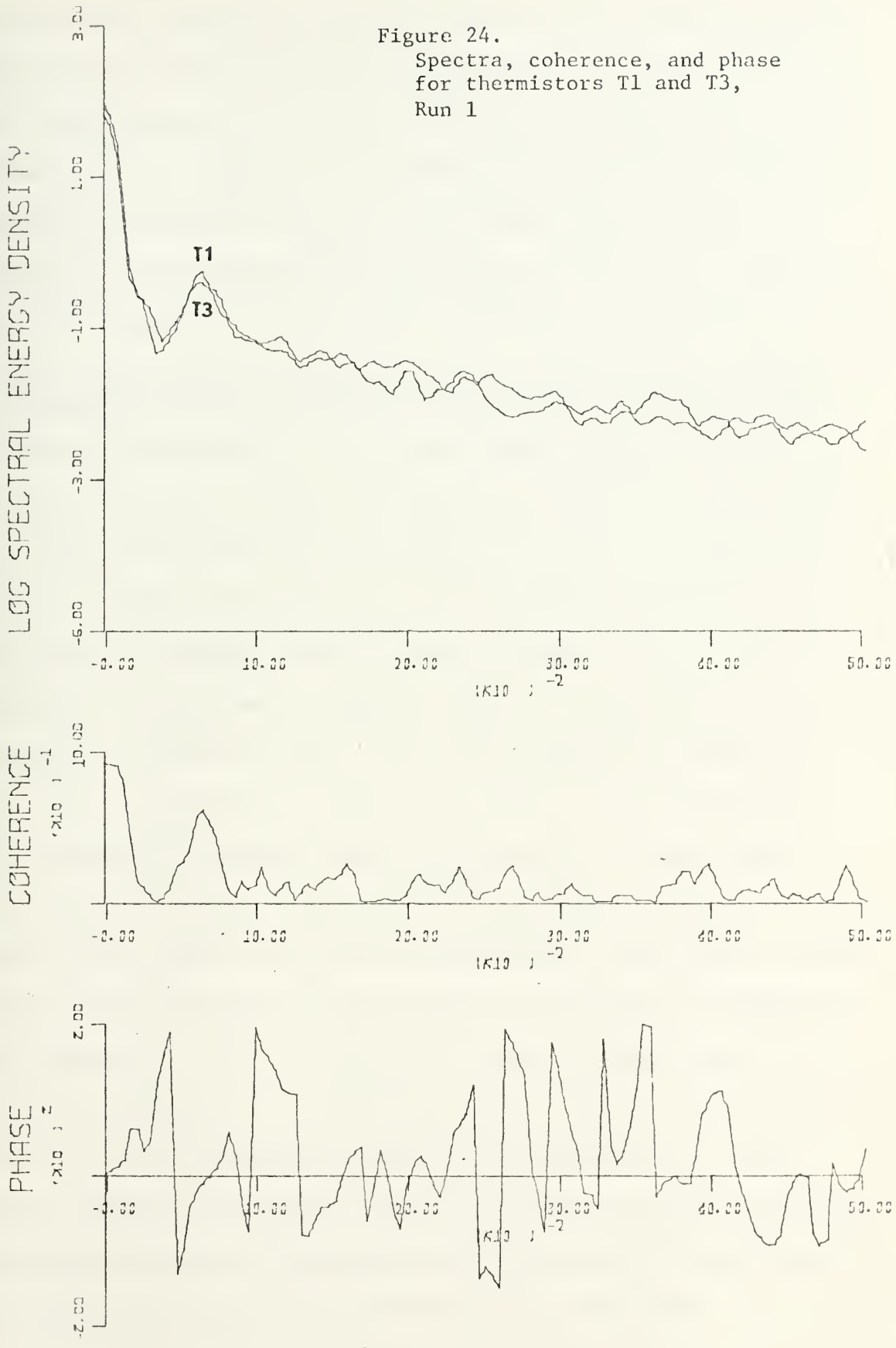

we assume that 14 seconds is the time required for an internal wave to travel from T1 to T3, than the average internal wave velocity is 6.35 cm/sec. which agrees fairly well with other data [Lafond (7)]. A second maximum value (.63) occurs in the coherence between T1 and T3 at the predominant wave frequency of .065 Hz. The energy density spectra of T1 and T3 are close to identical to a frequency of about .09 Hz. The fact that the coherence is less than one is attributed to turbulence.

D. RELATIONSHIP BETWEEN TEMPERATURE FLUCTUATIONS AND SOUND VELOCITY

Sensor T3 was located 23 cm from the sound velocimeter. Figure 25 is a plot of spectra, coherence and phase for T3 and sound velocity for Run 1. Fairly high values of coherence are apparent to a frequency of .12 Hz. At frequencies below about .01 Hz, coherence is close to 1.0 and T3 and sound velocity remain in phase to about .02 Hz. Near the predominant wave frequency, coherence reaches a value of .72 and phase is relatively constant at 36^{o} - 40^{o}. Little coherence is exhibited above .1 Hz. Figure 26 is a similar plot for T1 and sound velocity. T1 was located 66 cm farther away from the sound velocimeter than T3. In general the coherence between T1 and sound velocity is similar to that between T3 and sound velocity but at significantly lower levels. Below .01 Hz coherence is reduced to .92 and at the frequency of predominant waves coherence is .59. In addition, the band of frequencies in which temperature and sound velocity remain coherent is much narrower for T1 than for T3. The differences between the two temperature vs sound velocity coherence plots may be attributed to the existence of turbulent fluctuations between the two sensors or the fact that the time constants of the sound velocimeter and the thermistor were different.

Figure 25.
Spectra, coherence, and phase
for T3 and sound velocity,
Run 1

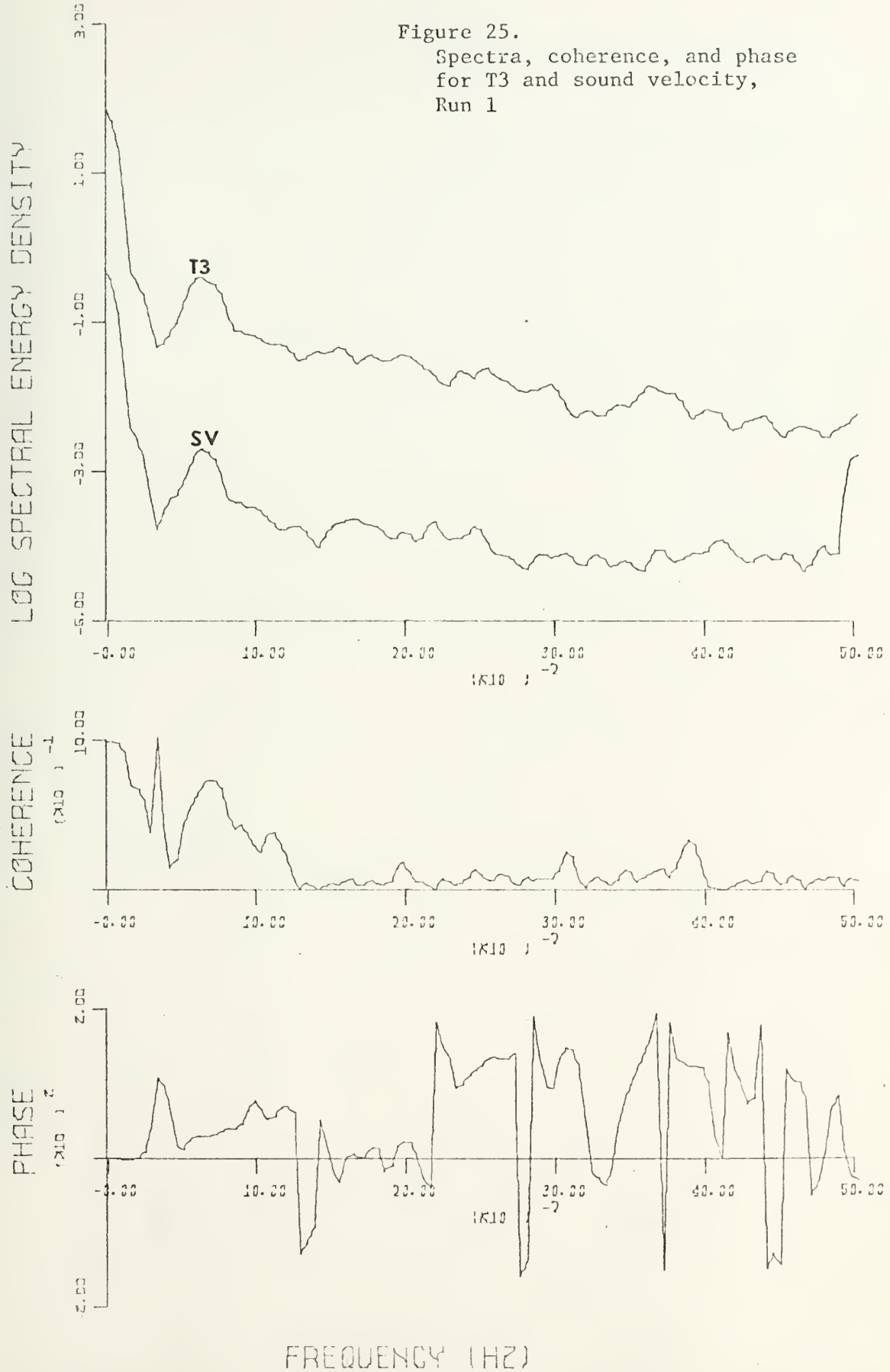

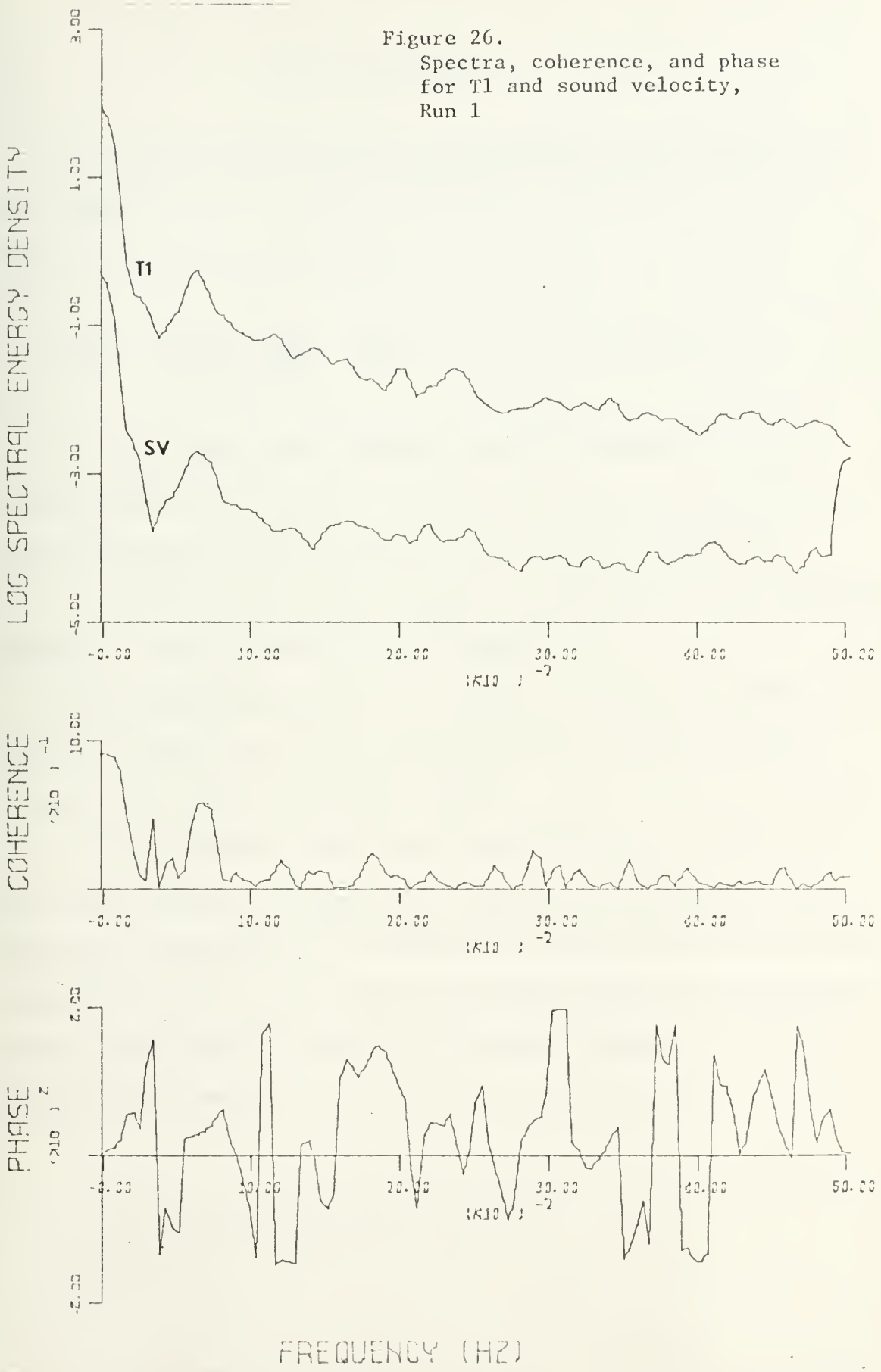

Figure 26.
Spectra, coherence, and phase for T1 and sound velocity, Run 1

VII. CONCLUSIONS

1. The relationship between temperature fluctuations and surface wave height (at least for swell-type waves) is verified to be of the form:

$$T(t) = K(f,z) \cdot \frac{dT}{dz} \cdot \eta(t)$$

2. All evidence points toward a similar relationship between internal waves and temperature fluctuations. Only one twenty minute record displayed sufficient internal wave activity to verify this.

3. Turbulent temperature fluctuations greatly degrade the coherence between two sensors located only 89 cm apart.

4. Further experimentation is needed to establish the relationship between non-swell surface waves and temperature fluctuations and to further verify the internal wave relation.

5. To successfully measure small scale spatial correlations of the temperature field, sensors must be placed at several points with separations less than 89 cm. Furthermore in order to do this with fast response thermistors a great deal of redundancy must be built into the system as this type of sensor has only marginal durability for oceanographic measurements.

LIST OF REFERENCES

1. Arthur, R. S., "Oscillations in Sea Temperature at Scripp's and Oceanside Piers", Deep Sea Research, Vol. 2, No. 2, pp. 107-121, 1954.

2. Bendat, J. S., and Piersol, A. G., Random Data: Measurement and Analysis Procedures, Wiley and Sons, 1971.

3. Cairns, J. L., and Nelson, K. W., "A Description of the Seasonal Thermocline Cycle in Shallow Coastal Water", Journal of Geophysical Research, Vol. 75, No. 6, pp. 1127-1131, 1970.

4. Frigge, W. F., "A Shallow Water Experiment with the STD Model 9006 at a Fixed Point", M.S. Thesis, U.S. Naval Postgraduate School, 1973.

5. Gossner, J., "Comparison of Measured and Calculated Sound Velocity Near the Sea Surface", M.S. Thesis, U.S. Naval Postgraduate School, 1973.

6. Krapohl, R. F., "Wave-Induced Water Particle Motion Measurements", M.S. Thesis, U.S. Naval Postgraduate School, 1972.

7. Lafond, E. C., and Lee, O. S., "Internal Waves in the Ocean", Navigation, Vol. 9, pp. 231-241, 1962.

8. Lafond, E. C., "Temperature Structure of the Upper Layer of the Sea and Its Variation with Time", Temperature, Its Measurement and Control in Science and Industry, Vol. 3, No. 1, pp. 751-767, 1962.

9. Liebermann, L., "The Effect of Temperature Inhomogenieties in the Ocean on the Propagation of Sound", Journal of the Acoustical Society of America, Vol. 23, pp. 563-571, 1951.

10. Shonting, D. H., and Kadis, A. L., "The Thermiprobe: A System for Measuring Thermal Microstructure in the Sea", Marine Sciences Instrumentation, Vol. 4, pp. 652-660, 1968.

11. Tennekes, H., and Lumley, J. L., A First Course in Turbulence, M.I.T. Press, 1972.

12. Urick, R. J., Lund, G. R., and Bradley, D. L., "Observations of Fluctuations of Transmitted Sound in Shallow Water", Journal of the Acoustical Society of America, Vol. 45, No. 3, pp. 683-690, 1969.

INITIAL DISTRIBUTION LIST

		No. Copies
1.	Defense Documentation Center Cameron Station Alexandria, Virginia 22314	2
2.	Library, Code 0212 Naval Postgraduate School Monterey, California 93940	2
3.	Oceanographer of the Navy The Madison Building 732 N. Washington Street Alexandria, Virginia 22217	1
4.	Department of Oceanography Naval Postgraduate School Monterey, California 93940	3
5.	Commander, Navy Ship Systems Command Code 901 Department of the Navy Washington, D. C. 20305	1
6.	Program Director, Physical Oceanography Code 481 Ocean Science and Technology Division Office of Naval Research Arlington, Virginia 22217	1
7.	LCDR Jon W. Carlmark (USN) Project Office Code 485 Ocean Science and Technology Division Arlington, Virginia 22217	1
8.	Professor H. Medwin, Code 61 Department of Physics Naval Postgraduate School Monterey, California 93940	1
9.	Dr. Noël E. Boston (thesis advisor) Code 58 Department of Oceanography Naval Postgraduate School Monterey, California 93940	3

INITIAL DISTRIBUTION LIST (continued)

		No. Copies
10.	Dr. E. B. Thornton Code 58 Department of Oceanography Naval Postgraduate School Monterey, California 93940	1
11.	LT Michael A. N. Whittemore, USN SMC 3003 Naval Postgraduate School Monterey, California 93940	2
12.	Director of Defense Research and Engineering Office of the Secretary of Defense Washington, D. C. 20301 ATTN: Office, Assistant Director (Research)	1
13.	Office of Naval Research Department of the Navy Arlington, Virginia 22217	
	ATTN: Ocean Science & Technology Division (Code 480)	3
	ATTN: Naval Applications & Analysis Division (Code 460)	1
	ATTN: Earth Sciences Division (Code 417)	1
14.	Director Naval Research Laboratory Washington, D. C. 20390	
	ATTN: Library, Code 2029 (ONRL)	6
	ATTN: Library, Code 2000	6
15.	Commander Naval Oceanographic Office Washington, D. C. 20390	
	ATTN: Code 1640 (Library)	1
	ATTN: Code 70	1
16.	Director National Oceanic and Atmospheric Administration National Oceanographic Data Center Washington Navy Yard Rockville, Maryland 20852	1

Unclassified

Security Classification

DOCUMENT CONTROL DATA - R & D

(Security classification of title, body of abstract and indexing annotation must be entered when the overall report is classified)

ORIGINATING ACTIVITY (Corporate author)

Naval Postgraduate School
Monterey, California 93940

2a. REPORT SECURITY CLASSIFICATION

Unclassified

2b. GROUP

REPORT TITLE

SMALL SCALE TEMPERATURE FLUCTUATIONS NEAR THE SEA SURFACE

DESCRIPTIVE NOTES (Type of report and, inclusive dates)

Master's Thesis; March 1973

AUTHOR(S) (First name, middle initial, last name)

Michael A. N. Whittemore

REPORT DATE	7a. TOTAL NO. OF PAGES	7b. NO. OF REFS
March 1973		12

CONTRACT OR GRANT NO.	9a. ORIGINATOR'S REPORT NUMBER(S)
PROJECT NO.	
	9b. OTHER REPORT NO(S) (Any other numbers that may be assigned this report)

DISTRIBUTION STATEMENT

Approved for public release; distribution unlimited.

SUPPLEMENTARY NOTES	12. SPONSORING MILITARY ACTIVITY
	Naval Postgraduate School Monterey, California 93940

ABSTRACT

Thermistor measurements of small scale temporal and spatial fluctuations of temperature were made near the surface of the sea from the NUC Oceanographic Research Tower. Wave height, water particle velocity, sound velocity, and salinity were measured simultaneously. Data were subjected to statistical and spectral analyses. Temperature fluctuations were found to vary with wave height. A linear relation was found to exist between temperature fluctuations and wave swell. The assumed relationship was verified by the results of spectral analysis. High coherence (.68) between wave height and temperature fluctuations occurred near the frequency of maximum wave energy. A relatively constant phase difference of 180° was observed in the frequency band normally associated with surface swell (.03 Hz to 0.2 Hz). Water particle velocities displayed the same relatively high coherence in the frequency band of high wave energy. Temperature fluctuations were 180° out of phase with the u-component of velocity and 90° out of phase with the w-component of velocity. These phase differences agreed with linear wave theory. Coherence was observed to be lower and phase difference more random with increased thermal gradients. This was attributed to an increase in turbulent temperature fluctuations.

DD FORM 1 NOV 65 1473 (PAGE 1)

S/N 0101-807-6811

Unclassified

Security Classification

A-31408

KEY WORDS	LINK A		LINK B		LINK C	
	ROLE	WT	ROLE	WT	ROLE	WT
TEMPERATURE FLUCTUATIONS, OCEANIC						
TEMPERATURE/WAVE HEIGHT RELATIONSHIP